Article

Cell Reports

BAX/BAK-Induced Apoptosis Results in Caspase-8-Dependent IL-1β Maturation in Macrophages

Graphical Abstract

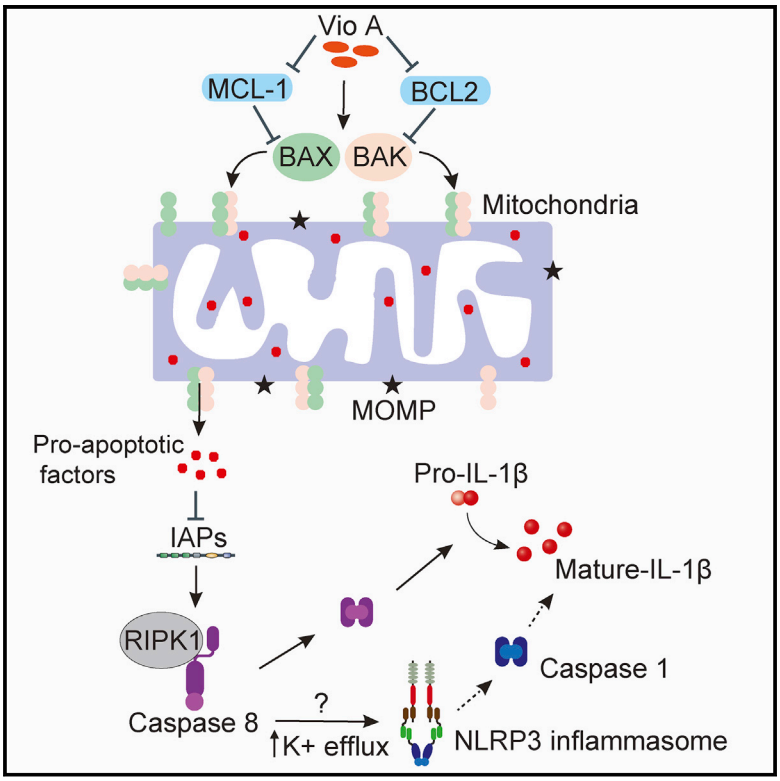

Authors

Dhruv Chauhan, Eva Bartok, Moritz M. Gaidt, ..., Stephen W.G. Tait, Rolf Müller, Veit Hornung

Correspondence

hornung@genzentrum.lmu.de

In Brief

Chauhan et al. provide insight into how intrinsic apoptosis can be connected to inflammation. In macrophages, mitochondrial apoptosis results in IAP depletion, which triggers caspase-8 activation. In this setting, caspase-8 is the main protease that matures the central pro-inflammatory cytokine IL-1β, while the NLRP3 inflammasome only plays a subordinate role.

Highlights

- Mitochondrial apoptosis is not a silent cell death pathway
- BAX/BAK-induced MOMP results in IL-1β maturation and lytic cell death
- MOMP initiates intrinsic apoptosis and IAP depletion
- This IAP depletion results in ripoptosome-caspase-8-dependent IL-1β maturation

Chauhan et al., 2018, Cell Reports *25*, 2354–2368
November 27, 2018
https://doi.org/10.1016/j.celrep.2018.10.087

CellPress

OPEN ACCESS
CellPress

Cell Reports
Article

BAX/BAK-Induced Apoptosis Results in Caspase-8-Dependent IL-1β Maturation in Macrophages

Dhruv Chauhan,[1,12] Eva Bartok,[2,12] Moritz M. Gaidt,[1] Florian J. Bock,[3,4] Jennifer Herrmann,[5,6,11] Jens M. Seeger,[7,8,9] Petr Broz,[10] Roland Beckmann,[1] Hamid Kashkar,[7,8,9] Stephen W.G. Tait,[3,4] Rolf Müller,[5,6,11] and Veit Hornung[1,13,*]

[1]Gene Center and Department of Biochemistry, Ludwig-Maximilians-Universität München, 81377 Munich, Germany
[2]Institute of Clinical Chemistry and Clinical Pharmacology, University Hospital, University of Bonn, 53127 Bonn, Germany
[3]Cancer Research UK Beatson Institute, University of Glasgow, Garscube Estate, Switchback Road, Glasgow G61 1BD, UK
[4]Institute of Cancer Sciences, University of Glasgow, Garscube Estate, Switchback Road, Glasgow G61 1BD, UK
[5]Department of Microbial Natural Products, Helmholtz Institute for Pharmaceutical Research Saarland (HIPS), Saarland University, 66123 Saarbrücken, Germany
[6]Helmholtz Centre for Infection Research and Department of Pharmacy, Saarland University, 66123 Saarbrücken, Germany
[7]Institute for Medical Microbiology, Immunology and Hygiene (IMMIH), University of Cologne, 50931 Cologne, Germany
[8]Center for Molecular Medicine Cologne (CMMC), University of Cologne, 50931 Cologne, Germany
[9]Cologne Excellence Cluster on Cellular Stress Responses in Aging-Associated Diseases (CECAD), University of Cologne, 50931 Cologne, Germany
[10]Department of Biochemistry, University of Lausanne, 1066 Epalinges, Switzerland
[11]German Center for Infection Research (DZIF), partner site Hannover-Braunschweig, 38124 Braunschweig, Germany
[12]These authors contributed equally
[13]Lead Contact
*Correspondence: hornung@genzentrum.lmu.de
https://doi.org/10.1016/j.celrep.2018.10.087

SUMMARY

IL-1β is a cytokine of pivotal importance to the orchestration of inflammatory responses. Synthesized as an inactive pro-cytokine, IL-1β requires proteolytic maturation to gain biological activity. Here, we identify intrinsic apoptosis as a non-canonical trigger of IL-1β maturation. Guided by the discovery of the immunomodulatory activity of vioprolides, cyclic peptides isolated from myxobacteria, we observe IL-1β maturation independent of canonical inflammasome pathways, yet dependent on intrinsic apoptosis. Mechanistically, vioprolides inhibit MCL-1 and BCL2, which in turn triggers BAX/BAK-dependent mitochondrial outer membrane permeabilization (MOMP). Induction of MOMP results in the release of pro-apoptotic factors initiating intrinsic apoptosis, as well as the depletion of IAPs (inhibitors of apoptosis proteins). IAP depletion, in turn, operates upstream of ripoptosome complex formation, subsequently resulting in caspase-8-dependent IL-1β maturation. These results establish the ripoptosome/caspase-8 complex as a pro-inflammatory checkpoint that senses the perturbation of mitochondrial integrity.

INTRODUCTION

Interleukin 1β (IL-1β) is a pleiotropic cytokine, which is crucial to orchestrating host defense against a variety of pathogens. At the same time, IL-1β has been shown to participate in the pathogenesis of many sterile inflammatory conditions (Dinarello, 2011). IL-1β is synthesized as a cytosolic precursor protein that requires cleavage for biological activity. Upon maturation, it is released into the extracellular space to exert its activity, a process that typically relies on the activation of macromolecular complexes known as inflammasomes (Broz and Dixit, 2016). Inflammasomes are high-molecular-weight cytoplasmic complexes formed in response to various microbial molecular patterns or perturbations of cellular homeostasis. In general, inflammasomes consist of a sensor protein (e.g., an NLR protein), the adaptor protein ASC (gene name *PYCARD*), and the protease caspase-1. Upon activation, the sensor protein seeds the prion-like multimerization of the adaptor ASC through homotypic pyrin domain (PYD) interactions, which induce the formation of large ASC filament structures. This in turn results in the recruitment of caspase-1, which itself is then activated by proximity-induced auto-cleavage. Active caspase-1 catalyzes the proteolytic maturation of IL-1β and its IL-1 family member IL-18 (Broz and Dixit, 2016). In addition to its cytokine substrates, caspase-1 cleaves the cell death effector molecule gasdermin D (GSDMD), which results in the formation of a pore in the plasma membrane, triggering a form of cell death known as pyroptosis (Kayagaki et al., 2015; Liu et al., 2016; Shi et al., 2015). Mature IL-1β can gain access to the extracellular space in the context of pyroptosis or other types of cell death (Gaidt and Hornung, 2018). In addition, it can be released through GSDMD pores that form at the plasma membrane preceding cell disintegration (Evavold et al., 2018). However, under certain conditions, IL-1β can also be released from living cells, independently of GSDMD or pyroptosis (Conos et al., 2016; Gaidt et al., 2016).

Among all inflammasome sensor proteins, NLRP3 is the most studied to date because of its critical role in sterile inflammatory diseases. These include rare, monogenetic autoinflammatory diseases, in which gain-of-function mutations within NLRP3 cause autoactivation of the NLRP3 inflammasome, as well as common, stimulus-dependent modes of NLRP3 activation, as observed in gout, atherosclerosis, or Alzheimer's disease (Dinarello, 2011; Masters et al., 2009). Inflammasome-dependent IL-1β maturation is a two-step process, in which signal 1 serves as the priming signal, which is required to induce pro-IL-1β expression, and signal 2 constitutes the stimulus that activates the inflammasome sensor itself. In the case of the NLRP3 inflammasome, signal 1 additionally serves to facilitate NLRP3 activation at transcriptional and post-transcriptional levels (Bauernfeind et al., 2009; Juliana et al., 2012). While the exact mechanism of NLRP3 activation remains unclear, a link has been established between most of the currently known NLRP3 stimuli and the lowering of cytoplasmic K^+ levels. Moreover, decreases in intracellular K^+ are known to be sufficient for NLRP3 activation (Franchi et al., 2007; Pétrilli et al., 2007). Given the fact that K^+ efflux readily occurs along its electrochemical gradient when the integrity of plasma membrane is breached, NLRP3 can be considered a sensor of membrane perturbation (Gaidt and Hornung, 2018). In addition, it has been proposed that loss of mitochondrial integrity leading to the release of mitochondrial damage-associated molecular patterns (DAMPs) can trigger NLRP3 inflammasome activation (Iyer et al., 2013; Shimada et al., 2012). These studies have demonstrated evidence for a mechanism in which mitochondrial DAMPs are released downstream of K^+ efflux and upstream of NLRP3 activation. However, this concept was challenged by genetic models in which the inhibition of mitochondrial DAMP release had no effect on canonical NLRP3 activation (Allam et al., 2014).

Apart from caspase-1, other enzymes have been shown to be capable of IL-1β maturation. This includes enzymes that can cleave IL-1β in the extracellular space, such as neutrophil-derived proteases, or caspase-8, which can process IL-1β in a cell-intrinsic fashion like caspase-1(Afonina et al., 2015; Maelfait et al., 2008). To date, several pathways leading to caspase-8-mediated IL-1β maturation have been described. One such pathway is the activation of caspase-8 in the context of ripoptosome formation that leads to IL-1β cleavage (Lawlor et al., 2015; Vince et al., 2012). The ripoptosome is a caspase-8-activating signaling hub that is formed by receptor-interacting serine/threonine-protein kinase 1 (RIPK1) under certain conditions, where it is able to recruit Fas-associated death domain (FADD) and subsequently caspase-8. Here, a key checkpoint function has been ascribed to the E3 ubiquitin ligases cellular inhibitor of apoptosis 1 (cIAP1), cIAP2, and, under certain conditions, XIAP (referred to in the following as IAPs). In the context of Toll-like receptor- (TLR-) and tumor necrosis factor receptor 1- (TNFR1-) dependent signaling cascades, IAPs ubiquitinate, among other targets, RIPK1, allowing it to engage in nuclear factor κB (NF-κB) activation and preventing it from forming a ripoptosome complex (Feoktistova et al., 2011; Tenev et al., 2011). However, in the absence of IAPs, de-ubiquitinated RIPK1 initiates the formation of a ripoptosome complex, which can act independently of an additional upstream signal. Thus, treating cells with compounds that deplete IAPs leads to the formation of a caspase-8-activating ripoptosome complex. Using this model system, it has been shown that TLR-primed macrophages cleave IL-1β in a caspase-8-dependent manner (Lawlor et al., 2015; Vince et al., 2012). However, a physiological role for this type of IL-1β maturation has not been identified to date.

RESULTS

The Vioprolide Family of Cyclic Peptolides Induces IL-1β Release

To identify thus-far uncharacterized immunostimulatory compounds, a library of 259 natural small molecules purified from myxobacteria was screened for its capacity to induce IL-1β release from a murine macrophage cell line (Surup et al., 2018). This library was chosen because myxobacteria are known for their structurally diverse secondary metabolites that have only scarcely been explored for their biological activity (Herrmann et al., 2017). Our analysis identified vioprolide A (Vio A) as an inducer of IL-1β release. Vio A belongs to a class of cyclic peptolides, the vioprolides (Figure S1A), isolated from the myxobacterium *Cystobacter violaceus* (Schummer et al., 1996). While vioprolides are known to have antifungal properties and demonstrate cytotoxicity in eukaryotic cells (Schummer et al., 1996; Weissman and Müller, 2010), their mode of action remains unknown, and a role in IL-1β activation has not been reported to date (Bollati-Fogolin and Müller, 2008). To test the IL-1β-inducing capacity of Vio A in primary cells, we stimulated primary murine BMDMs (bone marrow-derived macrophages) (Figure 1A) and human PBMCs (peripheral blood mononuclear cells) (Figure 1B) with Vio A, while nigericin and double-stranded DNA (dsDNA) were included as controls to stimulate the NLRP3 or the absent in melanoma 2 (AIM2) inflammasome, respectively. Vio A triggered IL-1β release in both cell populations in a dose-dependent manner, but to a lesser extent than nigericin or dsDNA. The other known members of the vioprolide family, vioprolides B, C, and D (Figure S1), also induced IL-1β release, with Vio A and Vio B being the most potent activators (Figure 1C). Of note, as observed for nigericin, vioprolide treatment also resulted in lactate dehydrogenase (LDH) release, which is indicative of a lytic form of cell death (Figure 1D). To determine whether stimulation with vioprolides resulted in the proteolytic activation of IL-1β in addition to its release, the cellular supernatants and lysates of vioprolide-treated wild-type (WT) BMDMs were probed for cleaved caspase-1 and IL-1β via immunoblotting. In line with the positive control nigericin, vioprolides A, B, C, and D induced the release of fully mature IL-1β (17 kDa) and caspase-1 (20 kDa) into the cellular supernatant (Figure 1E). Thus, our data demonstrate that vioprolides are a family of cyclic peptides that are capable of inducing caspase-1 and IL-1β activation.

Vioprolides Induce IL-1β Release and Cell Death via NLRP3-Dependent and -Independent Mechanisms

To elucidate the pathway of vioprolide-mediated IL-1β maturation and LDH release, we stimulated WT BMDMs and cells deficient for the inflammasome components NLRP3, ASC, and caspase-1/11 with Vio A and Vio B, as well as with nigericin and dsDNA. In WT macrophages, stimulation with Vio A and Vio B

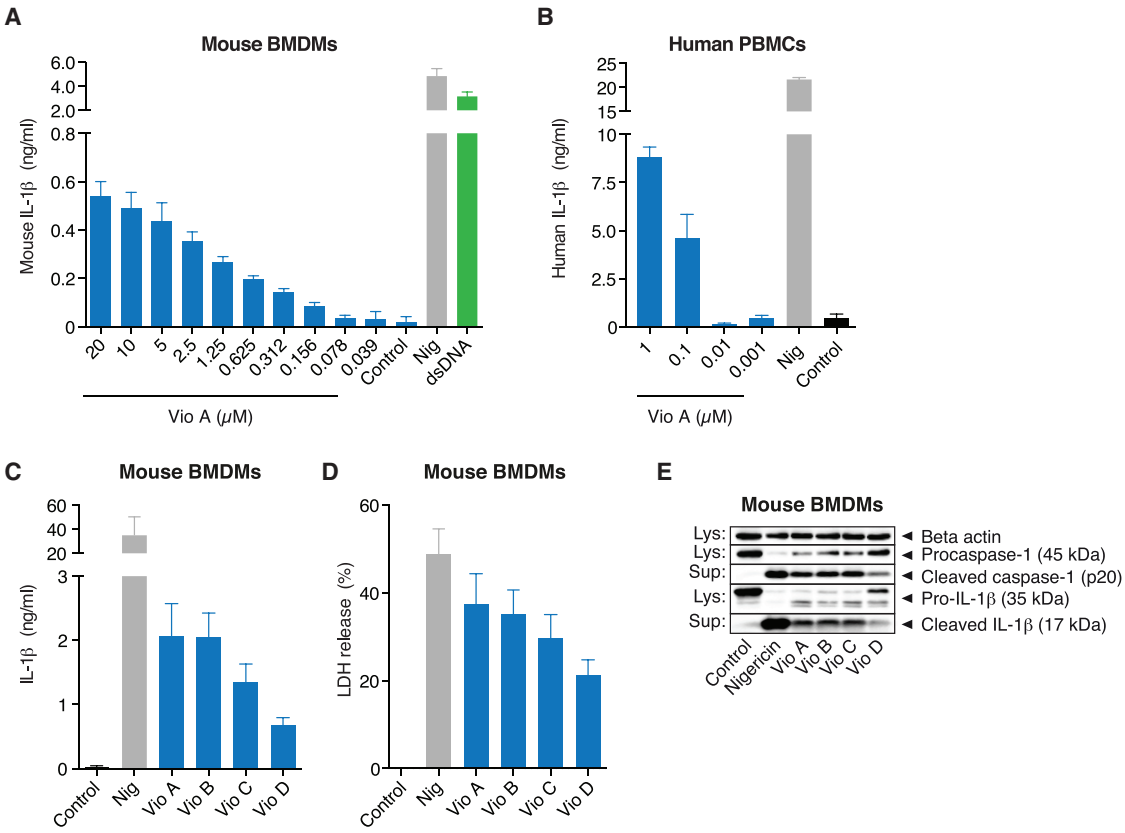

Figure 1. The Vioprolide Family of Cyclic Peptolides Induces IL-1β Release

(A) Wild-type (WT) BMDMs were primed with LPS (200 ng/mL) for 4 hr and stimulated with indicated concentrations of Vio A (in μM), nigericin, and dsDNA for 8 hr.

(B) Human PBMCs primed with LPS (50 pg/mL) for 4 hr and followed by stimulation with different concentrations of Vio A (in μM) and nigericin for 6 hr.

(C–E) LPS-primed WT BMDMs treated with nigericin and 20 μM of Vio A, B, C, and D for 8 hr. Samples were analyzed for (C) IL-1β release via ELISA and tested for (D) LDH activity in cellular supernatant and (E) immunoblot.

Data are depicted as mean + SEM of (A) four, (B) two (C and D) three or one representative blot of (E) three independent experiments. Sup, supernatant; Lys, lysate.

See also Figure S1.

resulted in the dose-dependent release of cleaved IL-1β (Figures 2A and S2A), as well as LDH (Figures 2B and S2E). While vioprolide-mediated IL-1β maturation and LDH release were largely unaffected by NLRP3, ASC, or caspase-1/11 deficiency (Figures 2A, 2B, S2A–S2H, and S3A–S3D), caspase-1 maturation was fully abrogated in NLRP3- and ASC-deficient BMDMs (Figures S3B and S3C). The control stimuli nigericin and dsDNA acted as expected in regard to their NLRP3, ASC, and/or caspase-1 dependence (Figure 2A). It should be noted that lytic cell death and its surrogate marker LDH release upon NLRP3 stimulation is caspase-1 dependent at early time points, but executed by caspase-1-independent mechanisms in *Casp1*$^{-/-}$ cells at later time points (Figures S3E–S3G) (Antonopoulos et al., 2015). Moreover, we also studied the role of the pyroptosis effector molecule GSDMD, which has been shown to mediate cell death and IL-1β release downstream of inflammasome activation (Kayagaki et al., 2015; Shi et al., 2015). As expected, BMDMs deficient in GSDMD showed a marked delay in IL-1β and LDH release after NLRP3 inflammasome stimulation (Figures 2C and 2D), yet Vio A-dependent LDH release was unaffected by GSDMD deficiency. Furthermore, while Vio A stimulation resulted in IL-1β and LDH release by different TLR ligands, including lipopolysaccharide (LPS) (Figure 2E), Vio A-induced LDH release occurred even in the absence of any TLR ligands (Figure 2F). Thus, our data demonstrate that vioprolides activate both NLRP3 inflammasome-dependent and -independent pathways. However, the maturation and release of IL-1β and the induction of cell death are largely independent of inflammasome components and GSDMD.

Vio A Triggers BAX- and BAK-Dependent Intrinsic Apoptosis, Resulting in IL-1β and LDH Release

At this point, our results raised the following questions: which caspase-1-independent cell death program is triggered by vioprolides, and how do vioprolides trigger the maturation and release of IL-1β? At the same time, what mechanism results in vioprolide-dependent activation of the NLRP3 inflammasome? To address the first question, we went on to further characterize the cell death induced by vioprolide exposure. To this end, we performed a DNA laddering assay, which revealed that Vio A

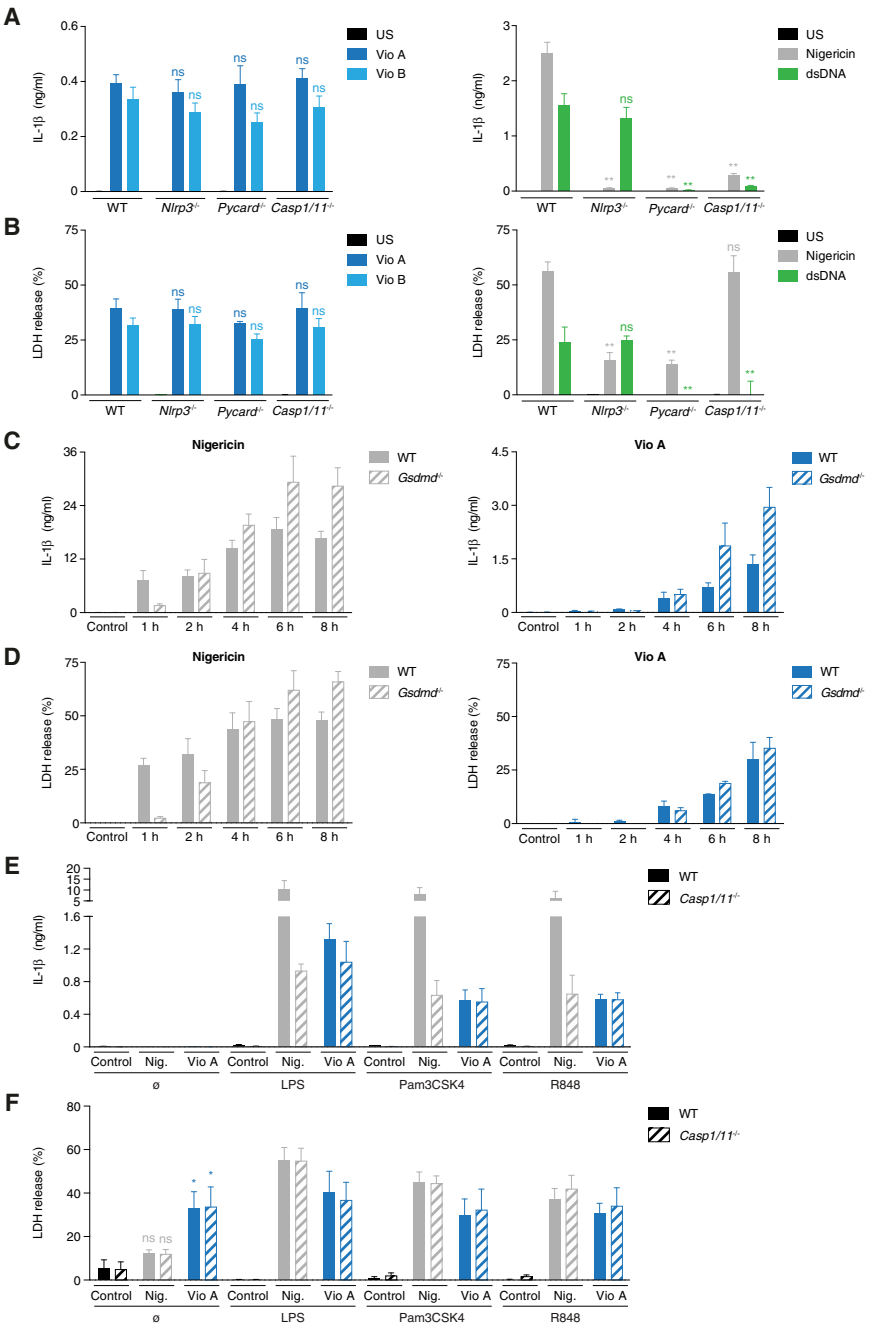

Figure 2. Vioprolides Induce IL-1β Release and Cell Death via NLRP3-Dependent and -Independent Mechanisms

(A and B) BMDM samples deficient in various inflammasome proteins were primed with LPS (200 ng/mL) for 4 hr and followed by 20 μM of Vio A and Vio B. Nigericin and dsDNA were used as controls. Cellular supernatants were assessed by (A) IL-1β ELISA and (B) LDH release after 8 hr.

(C and D) IL-1β (C) and LDH measurement (D) in the cellular supernatants of LPS-primed WT and *Gsdmd*$^{-/-}$ BMDMs stimulated with nigericin and Vio A for the indicated time points.

(E and F) WT and *Casp1/11*$^{-/-}$ BMDMs were primed with or without different TLR ligands for 4 hr (LPS: 200 ng/mL, Pam3CSK4: 2.5 μg/mL, R848: 2 μg/mL). Priming was followed by stimulation of Vio A and nigericin for 8 hr; cellular supernatants were analyzed for (E) IL-1β via ELISA and (F) LDH activity.

Error bars represent mean + SEM of (A and B) four, (C and D) two, and (E and F) three independent experiments. *p < 0.05, **p < 0.01, ns, not significant. Either individual genotypes were compared to the WT genotype or individual conditions were compared to the respective unstimulated control. See also Figures S2 and S3.

stimulation induced DNA fragmentation, a hallmark of apoptosis (Figures 3A and S4A). Although LDH release is not considered characteristic for apoptotic cell death, it has been shown that apoptotic stimuli can also result in LDH release due to secondary necrosis at late time points (England et al., 2014). Therefore, to differentiate between apoptotic and lytic cell death, we performed a time course for caspase-3 activation and LDH release using the protein kinase inhibitor staurosporine (STS) as an apoptosis-inducing control (England et al., 2014). Here, differences in caspase-3 activation and LDH release could be observed. Whereas Vio A treatment resulted in early proteolytic processing of caspase-3 (120 min) (Figure 3B), LDH release took place at a later time point (6 hr) (Figure 3C). Furthermore, we also observed processing of the initiator caspase-9 within 60 min of Vio A treatment, which was in line with early caspase-3 activation (Figure 3B). As expected, STS induced caspase-9 and caspase-3 activation, as well as DNA laddering (Figures 3A and 3B). Moreover, as previously shown, STS induced LDH release at later time points (6 and 10 hr) (Figures 3C and S6D) (England et al., 2014; Shimada et al., 2012). Caspase-9 represents the initiator caspase involved in intrinsic apoptosis, which is activated by cytosolic cytochrome *c* released from mitochondria after mitochondrial outer membrane permeabilization (MOMP) (Elmore, 2007). To study its potential involvement, WT BMDMs were stimulated with Vio A, and cytosolic fractions were isolated at various time points. Cytosolic cytochrome *c* was detected upon exposure to Vio A within minutes after treatment and was followed by the activation of caspase-9 and caspase-3 (Figure 3B; data not shown), strongly suggesting that Vio A treatment leads to the induction of MOMP.

MOMP is controlled by anti-apoptotic B cell lymphoma 2 (BCL2) protein family members that inhibit the oligomerization of pro-apoptotic members BAX and BAK, which in turn induces the release of pro-apoptotic factors such as cytochrome *c* (Youle and Strasser, 2008). Thus, to investigate the role of the BCL2

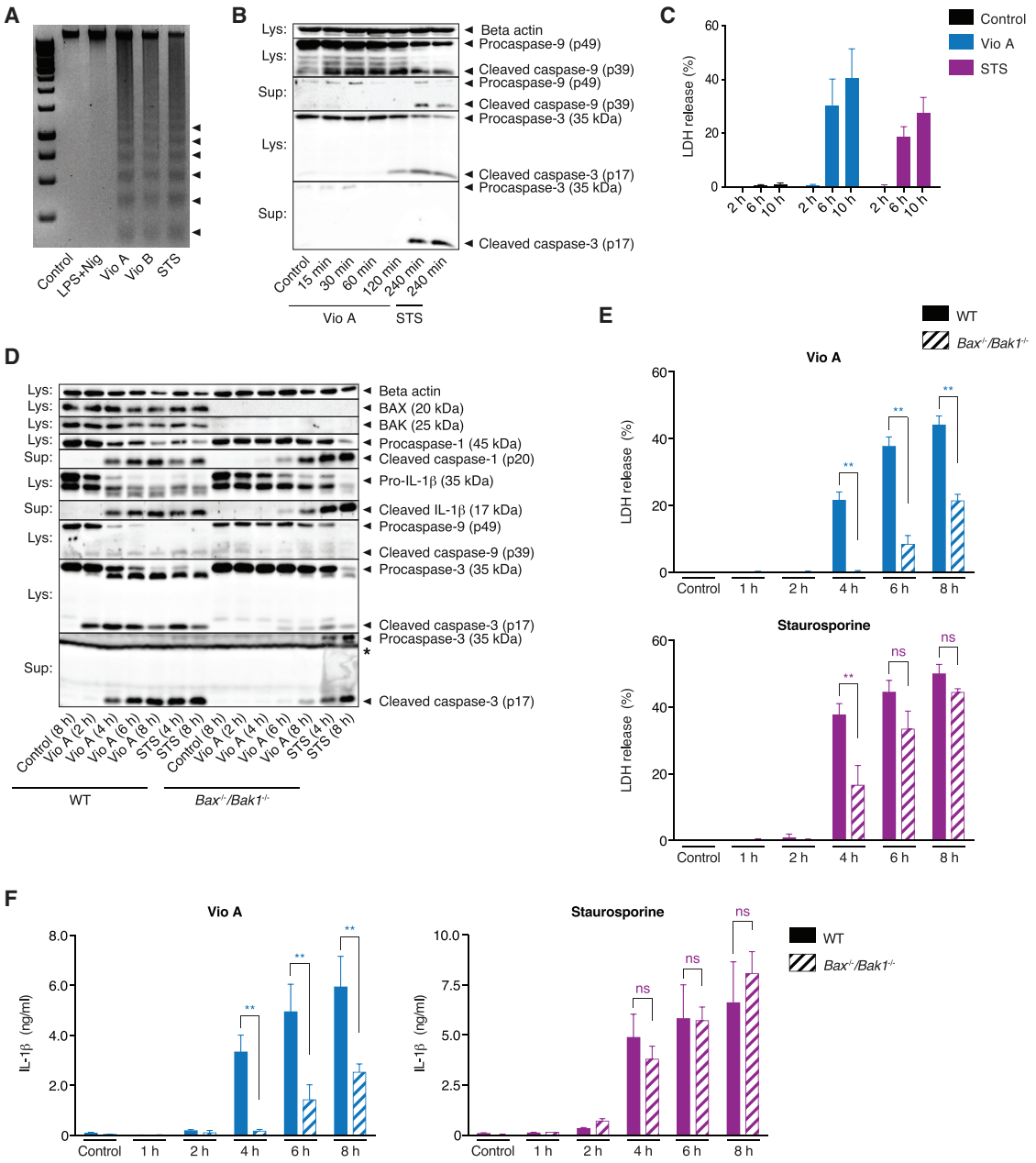

Figure 3. Vio A Triggers BAX- and BAK-Dependent Intrinsic Apoptosis, Resulting in IL-1β and LDH Release

(A) WT BMDMs were stimulated with Vio A and B for 6 hr and analyzed for DNA laddering. STS and LPS + nigericin were used as positive and negative controls, respectively. These data are representative of three independent experiments.

(B and C) WT BMDMs were treated with Vio A and STS, and samples were probed for (B) immunoblot and (C) LDH activity at indicated time points. Data are depicted as (B) one representative blot or (C) means + SEMs of three independent experiments.

(D–F) LPS primed WT and *Bax*$^{-/-}$/*Bak1*$^{-/-}$ BMDMs treated with Vio A and STS for the indicated time points. Samples were taken for (D) immunoblot at the indicated time points. In addition, cellular supernatants were analyzed for (E) LDH activity and (F) IL-1β via ELISA. Data are shown as (D) one representative blot or (E and F) mean + SEM of three independent experiments. *Non-specific cross-reactivity of the antibody. *$p < 0.05$, **$p < 0.01$, ns, not significant.

See also Figure S4.

protein family in Vio A-induced cell death, we used BAX- and BAK-deficient BMDMs. In comparison to WT cells, *Bax*$^{-/-}$/*Bak1*$^{-/-}$ cells demonstrated a marked delay in caspase-9 and caspase-3 activation after Vio A treatment (Figure 3D). Moreover, the deficiency of BAX and BAK both significantly delayed and reduced Vio A-induced LDH and IL-1β release (Figures 3E and 3F). However, compared to WT cells, *Bax*$^{-/-}$/*Bak1*$^{-/-}$ cells displayed an initial reduction in LDH release 4 hr after STS treatment

but not at later time points. Of note, in line with previous work, the deficiency of BAX and BAK had no impact on STS or nigericin-induced IL-1β maturation (Allam et al., 2014) (Figures 3F and S4B). Analogous results were observed when we studied macrophages that ectopically overexpress Bcl2 (OXP-BCL2) (Knittel et al., 2016). Compared to WT cells, OXP-BCL2 cells showed a marked decrease in LDH and IL-1β release when treated with vioprolides, while IL-1β and LDH release following nigericin stimulation remained unaffected (Figures S4C and S4D). This was paralleled by a strong decrease in vioprolide-mediated intrinsic apoptosis induction (caspase-9 and caspase-3 activation) in OXP-BCL2 cells (Figure S4D). As an additional control, we used the second mitochondria-derived activator of caspase (Smac) mimetic birinapant, which can trigger largely inflammasome-independent IL-1β maturation by IAP depletion (Lawlor et al., 2015; Vince et al., 2012) (Figures S4E and S4F). As expected, birinapant treatment readily induced LDH and IL-1β release, yet this response was only slightly affected by the overexpression of Bcl2. In summary, these results demonstrate that Vio A induces BAX- and BAK-dependent intrinsic apoptosis, leading to both IL-1β maturation and LDH release.

Vioprolides Act as Translational Inhibitors

Next, we wanted to explore how vioprolides trigger BAX/BAK activation upstream of MOMP. Pro-apoptotic Bcl-2 homology (BH) domain 3-only proteins induce MOMP by directly activating pro-apoptotic BAX/BAK and/or by antagonizing anti-apoptotic BCL2 proteins (Youle and Strasser, 2008). In macrophages, it has been shown that the depletion of the anti-apoptotic protein myeloid cell leukemia sequence 1 (MCL-1) plays a pivotal role in intrinsic apoptosis induction. However, MCL-1 depletion alone is not sufficient, and at least one additional signal is required to trigger MOMP in macrophages (Dzhagalov et al., 2007). Because intrinsic apoptosis was observed with Vio A treatment, WT BMDMs were tested for MCL-1 expression at the mRNA and protein levels after Vio A treatment (Figure 4A). MCL-1 is a short-lived protein that requires constant synthesis to maintain a stable expression level. Consequently, cycloheximide (CHX) and other translational inhibitors quickly decrease MCL-1 levels (Adams and Cooper, 2007). Although CHX treatment did not change MCL-1 transcript levels, Vio A treatment led to a marked increase in MCL-1 mRNA. Nonetheless, both CHX and Vio A treatment resulted in a substantial decrease in MCL-1 protein (Figure 4A), indicating that Vio A induces MCL-1 protein degradation at the post-transcriptional level. To investigate whether Vio A acts as a translational inhibitor *in vitro*, we used a eukaryotic cell-free translational system with mRNA encoding human hemoglobin subunit beta (HBB) (Matheisl et al., 2015). Cell-free translational extracts were incubated with Vio A and CHX for 40 min (Figure 4B) or DMSO as a control. In line with its ability to decrease MCL-1 levels in BMDMs, Vio A inhibited the translation of HBB in the cell-free system. The half-maximum inhibitory concentration (IC_{50}) was 112 nM for Vio A, while CHX displayed an IC_{50} of 945 nM.

Having established intrinsic apoptosis as the upstream activating pathway of Vio A-dependent IL-1β and LDH release, we investigated whether intrinsic apoptosis in general could induce these effects. To this end, LPS-primed BMDMs were cultured in the presence and absence of CHX to deplete MCL-1 and treated with the BCL2/BCL-X_L (B cell lymphoma-extra large) inhibitor ABT-737 (Oltersdorf et al., 2005) (Figure 4C). As expected, ABT-737 treatment alone was not sufficient for the induction of intrinsic apoptosis, and no activation of caspase-3 or caspase-9 was observed. Thus, ABT-737 treatment alone also did not induce the maturation of IL-1β or caspase-1. However, when combined with CHX to induce MCL-1 depletion, ABT-737 could trigger intrinsic apoptosis, as well as the maturation of IL-1β and caspase-1. Conversely, in line with our previous data, CHX treatment was not required for Vio A-dependent IL-1β maturation and caspase-1 activation (Figure 4C). Similar to Vio A, CHX + ABT-737-induced IL-1β was largely independent of NLRP3 (Figure S5A). Furthermore, the proteasomal inhibitor MG-132 could slightly restore MCL-1 levels in Vio A-treated cells, which is in line with previous reports of proteasomal degradation of MCL-1 (Adams and Cooper, 2007). Stabilizing MCL-1 levels via MG-132 delayed the kinetics of Vio A-dependent apoptosis and IL-1β maturation (Figure S5B). These data indicate that vioprolides act as translational inhibitors, thus decreasing the protein levels of the crucial pro-survival BCL2 family member MCL-1. At the same time, vioprolides appear to confer an additional pro-apoptotic signal upstream of BAX/BAK. The combination of both functionalities then triggers MOMP in macrophages (Figure 4D). Accordingly, these events can be mimicked by the combination of a translational inhibitor (CHX) that depletes MCL-1 and a BCL2/BCL-X_L antagonizing compound.

Vioprolides Inhibit Pro-survival BCL2

To identify the second trigger activated by vioprolides, we used the previously described mito-priming method (Lopez et al., 2016). In brief, in this method, seminal vesicle epithelial cells (SVECs) are rendered ''addicted'' to specific BCL2 proteins via the constitutive co-expression of an anti-apoptotic and a pro-apoptotic protein. This configuration makes them dependent on the specific BCL2 protein for their survival. We treated BCL2, BCL-X_L, and MCL-1 mito-primed cell lines with vioprolides and tracked their survival in a time course experiment via a SYTOX green exclusion assay; BCL2-, BCL-X_L-, and MCL-1-specific inhibitors served as specificity controls, whereas the combined treatment of ABT-737 + actinomycin D was used as a pro-apoptotic stimulus that was active across all three cell lines. Vioprolides specifically resulted in the death of BCL2-dependent cells, while BCL-X_L-dependent cells were completely unaffected by vioprolide treatment (Figures 5A, 5B, S5C, S5D, and S5F). Moreover, vioprolide treatment also resulted in the death of MCL-1-dependent cells (Figures 5C, S5E, and S5F). Taken together with our data on BCL2 overexpression (Figures S4C and S4D) and MCL-1 depletion (Figures 4A and 4C), these findings confirm that vioprolides inhibit MCL-1 and BCL2, providing two distinct triggers to initiate BAX/BAK-dependent MOMP (Figure S5G).

Caspase-8 Is the Main Protease Catalyzing IL-1β Maturation during Intrinsic Apoptosis

While our results thus far strongly suggested that intrinsic apoptotic machinery mediates the cleavage of IL-1β independently of caspase-1, the respective protease remained elusive. In addition to cytochrome *c* release, MOMP triggers the release

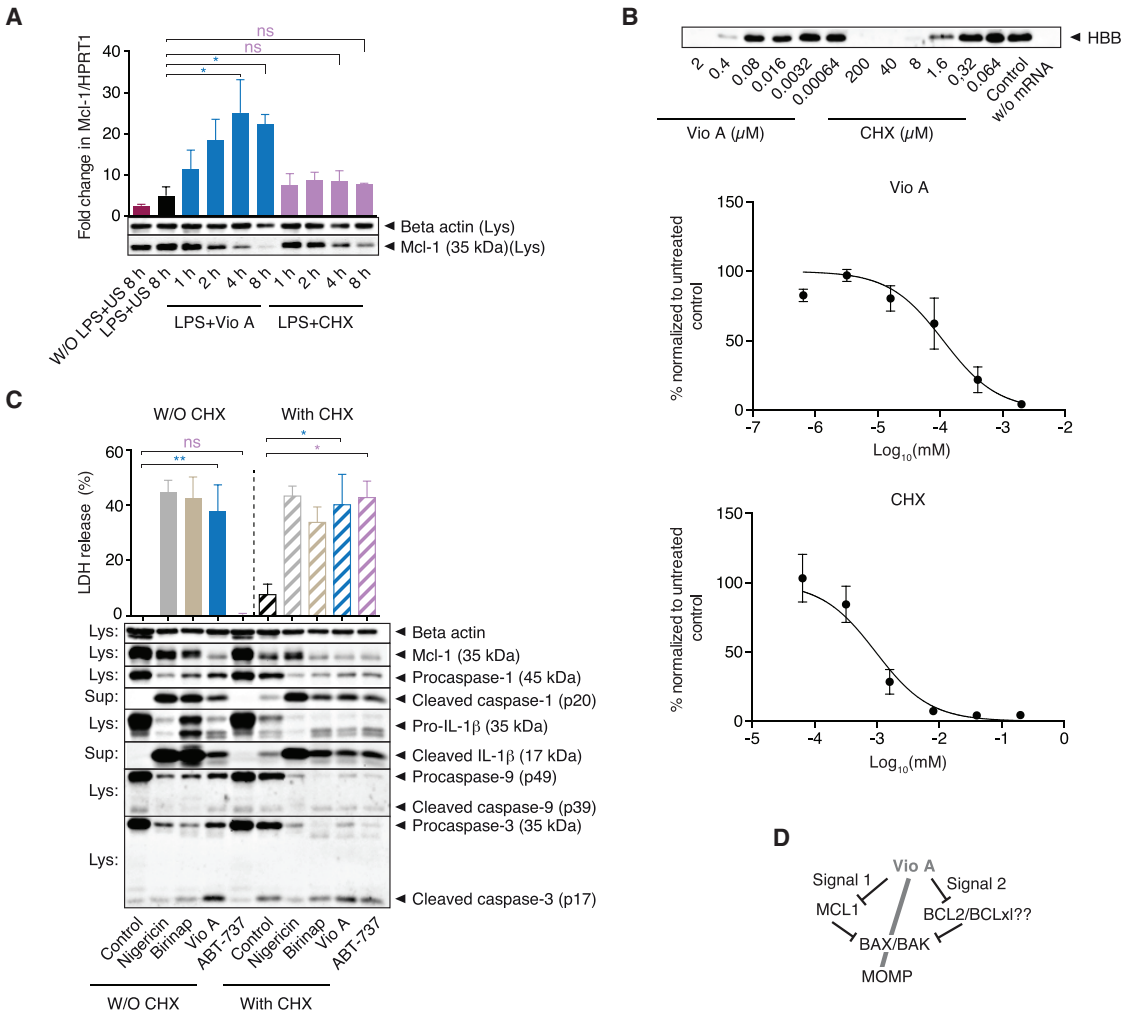

Figure 4. Vioprolides Act as Translational Inhibitors

(A) WT BMDMs treated with or without LPS for 4 hr and followed by stimulation with Vio A and cycloheximide (CHX) for the indicated time points. Samples were analyzed for Mcl-1 expression at mRNA level (top) and protein level (bottom).

(B) Immunoblot of cell-free translational assay for human HBB mRNA in the presence and absence of the indicated concentrations of Vio A and CHX for 40 min. DMSO control was used for maximum translation, while translational extract without mRNA was used as negative control and for background normalization. For IC_{50} determination, curve fitting was performed with non-linear regression with log(inhibitor) versus normalized response parameter logistic. Data are mean + SEM or one representative blot of three independent experiments.

(C) WT BMDMs were primed with LPS for 4 hr and stimulated with nigericin, birinapant, Vio A, and ABT-737 in the presence and absence of CHX. CHX was added in the last 45 min of priming. Samples were taken after 8 hr for LDH release (top) and immunoblot (bottom).

(D) Schematic representation of Vio A-induced MOMP.

(A and C) One representative blot of three independent experiment. Error bars represent mean + SEM of three independent experiments. *$p < 0.05$, **$p < 0.01$, ns, not significant.

See also Figure S5.

of other pro-apoptotic factors such as SMAC/DIABLO (direct inhibitor of apoptosis-binding protein with low isoelectric point) and mitochondrial serine protease HTRA2 (HtrA2), which antagonize IAP proteins (Elmore, 2007). In the context of MOMP, it is well established that IAP depletion can amplify apoptotic signaling cascades. However, using synthetic compounds, it has also been shown that depleting IAPs can trigger ripoptosome-dependent caspase-8 activation, leading to direct IL-1β maturation (Lawlor et al., 2015; Vince et al., 2012). Whether the latter pathway is operational in the context of MOMP has not yet been addressed. In the light of these considerations, we investigated whether Vio A triggers the release of pro-apoptotic factors from mitochondria that antagonize IAPs. To this end, unprimed WT BMDMs were treated with Vio A, and cytosolic fractions were isolated at different time points. Cytochrome *c* was detected in the cytosol within 15 min of Vio A treatment, and its levels increased further with time (Figure 6A). In addition to cytochrome *c*, the pro-apoptotic factor SMAC was also detected in the cytosolic fraction 2 hr after stimulation. Its release correlated with the depletion of all three IAPs tested, predominantly cIAP2 (Figure 6A). Next, we

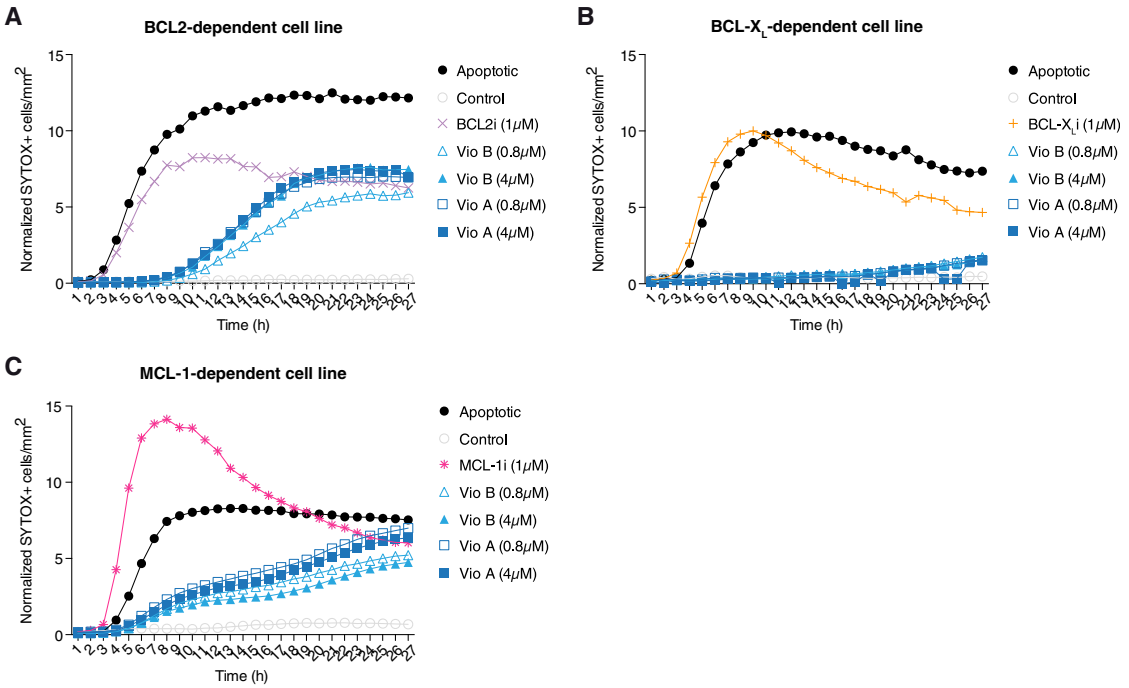

Figure 5. BCL2 Inhibition Confers Second Trigger for BAX/BAK-Dependent MOMP

(A–C) BCL2- (A), BCL-X_L- (B), and MCL-1- (C) dependent SVEC cells were treated with the indicated stimuli for the indicated time points. Cell death was analyzed by SYTOX green$^+$ cells/mm^2 and normalized to the initial confluency of respective wells. Data are representative of three independent experiments. See also Figure S5.

probed for the activation of caspase-8 in the supernatants of Vio A-treated samples, and depletion of all three IAPs correlated with an increase in caspase-8 activation. Moreover, in line with the aforementioned concept of IAP depletion and subsequent caspase-8 activation downstream of MOMP, BAX/BAK deficiency markedly delayed the depletion of IAPs and caspase-8 activation. Of note, MCL-1 degradation was independent of BAX and BAK, thus positioning it upstream of MOMP (Figure S6A). Similar observations were made in OXP-BCL2 macrophages. Overexpression of BCL2 prevented degradation of all three tested IAPs, and a reduced activation of caspase-8 after vioprolide treatment was observed (Figure S6B). As previously reported, STS treatment also resulted in the activation of caspase-8 (Figure 6A) (Antonopoulos et al., 2013). However, the mechanism of STS-dependent caspase-8 activation differed from Vio A in that it occurred independently of BAX and BAK, thereby excluding MOMP as the driving force (Figure S6A).

To determine whether caspase-8 is directly involved in Vio A-mediated IL-1β processing, we studied IL-1β maturation in *Casp8*$^{-/-}$/*Ripk3*$^{-/-}$ and *Ripk3*$^{-/-}$ BMDMs. Because genetic deficiency of caspase-8 alone is lethal in mice due to the engagement of the necroptotic pathway, caspase-8 deficiency can only be investigated in an *Ripk3*- or *Mlkl*-deficient background (Dillon et al., 2014; Kaiser et al., 2011; Oberst et al., 2011). As expected, treatment with the Smac mimetic birinapant resulted in mature IL-1β and LDH release from WT cells, which was completely dependent on ripoptosome-mediated caspase-8 activation (Figure 6B) (Lawlor et al., 2015). In contrast, nigericin could still induce IL-1β maturation in *Casp8*$^{-/-}$/*Ripk3*$^{-/-}$ cells, although IL-1β and LDH release were slightly reduced (Figure 6B). However, it should be noted that deficiency in caspase-8 also leads to defects in NF-κB signaling (Allam et al., 2014), which we could only partially compensate for with higher doses of LPS (Figure S6C). In contrast, Vio A-mediated IL-1β release was completely dependent on caspase-8, and LDH release was substantially reduced compared to WT cells. Because caspase-8 can initiate intrinsic apoptosis via BH3-interacting domain death agonist (BID) (Elmore, 2007), we additionally studied BID cleavage and the activation of caspase-9 and caspase-3 after Vio A stimulation in *Casp8*$^{-/-}$/*Ripk3*$^{-/-}$ and *Ripk3*$^{-/-}$ BMDMs (Figure 6C). However, *Casp8*$^{-/-}$/*Ripk3*$^{-/-}$ still showed activation of intrinsic apoptosis after Vio A treatment, demonstrating that vioprolides induce intrinsic apoptosis independently and thus upstream of caspase-8 (Figures 3B and 6C). These results were also in line with the fact that caspase-3 activation preceded the activation of caspase-8 in Vio A-treated cells (Figure S6D). Because we had observed IAP depletion before caspase-8 activation (Figure 6A), we additionally determined levels of cIAP1, cIAP2, and XIAP in *Casp8*$^{-/-}$/*Ripk3*$^{-/-}$. Vio A treatment resulted in the depletion of all three IAPs independently of caspase-8 (Figure 6C). In contrast, the Smac mimetic birinapant induced the degradation of cIAP2 and XIAP in a caspase-8-dependent manner (Figure 6C). Of note, treatment of CHX + ABT-737 and Vio A showed a similar pattern of IL-1β and LDH release. However, the kinetics of IL-1β and LDH release were faster for CHX + ABT-737 as compared to Vio A (Figures S6E and S6F).

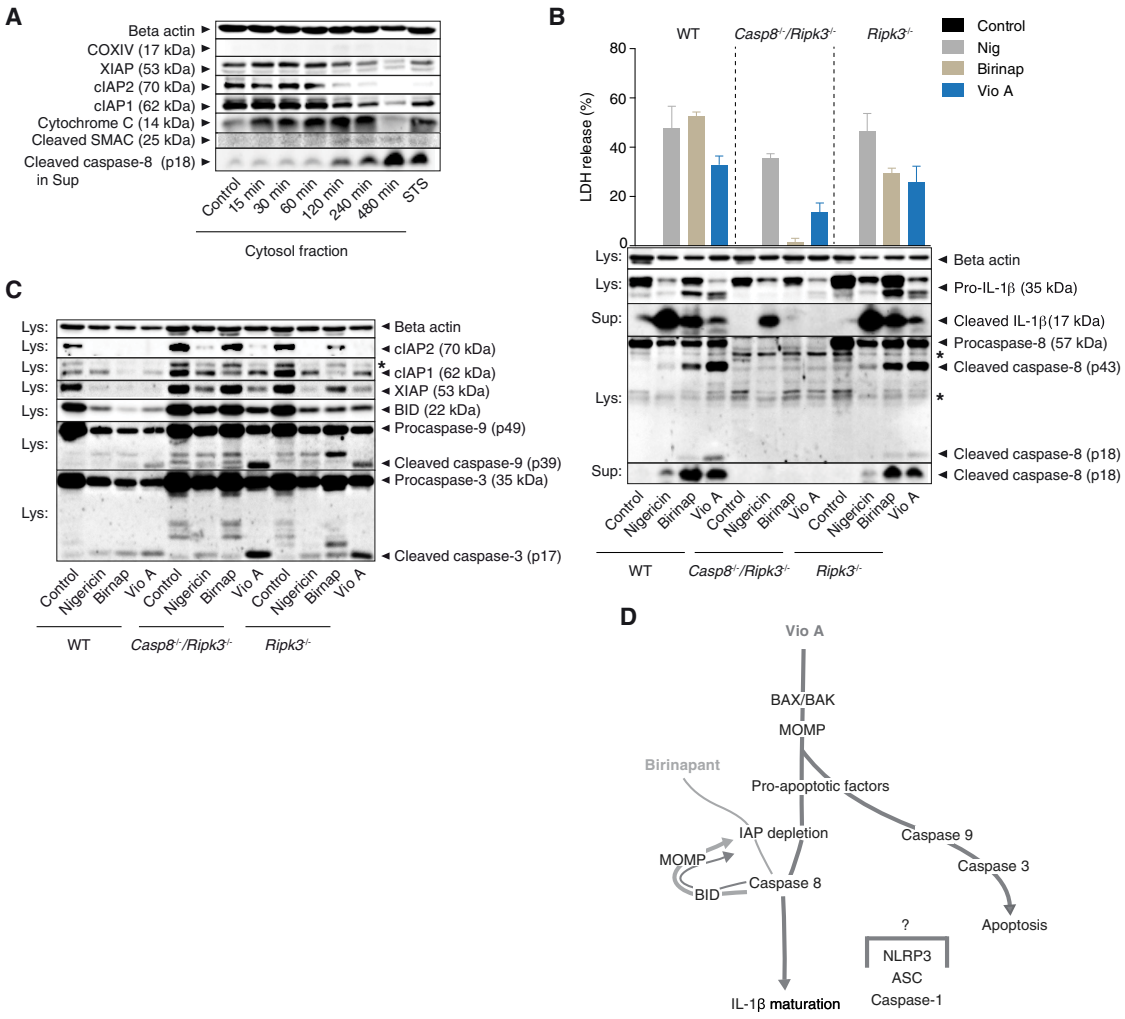

Figure 6. Caspase-8 Is the Main Protease in IL-1β Maturation during Intrinsic Apoptosis

(A) Immunoblot of cytosolic fractions of unprimed WT BMDMs treated with Vio A for different time points. STS (4 hr) was used as a control for cytochrome *c* release.

(B and C) WT, *Casp8*$^{-/-}$/*Ripk3*$^{-/-}$ and *Ripk3*$^{-/-}$ BMDMs primed with 1000 ng/mL LPS for 4 hr followed by stimulation with nigericin, birinapant, and Vio A for 8 hr. Samples were assessed for (B) LDH activity (top) and probed for (B and C) immunoblot.

(D) Schematic representation of Vio A and birinapant signaling pathway, in which the thick line represents strong signal, while the thin line represents weak signal.

Data are depicted as (A–C) one representative blot or (B) mean + SEM of two independent experiments. *Non-specific cross-reactivity of the antibody.

See also Figure S6.

In summary, these results indicated that vioprolide-triggered MOMP results in the release of pro-apoptotic factors, which in turn deplete IAPs. This leads to the activation of caspase-8 that directly matures IL-1β. While birinapant-mediated caspase-8 activation bypasses the need for MOMP induction, it still requires MOMP to fully deplete IAPs, creating a feedback loop for maximal caspase-8 activation (Figure 6D).

Intrinsic Apoptosis Results in Ripoptosome-Caspase-8-Dependent and -Independent NLRP3-Caspase-1 Activation

The delay in intrinsic apoptosis also correlated with a delay in Vio A-dependent caspase-1 activation, indicating that NLRP3-inflammasome activation in response to Vio A is secondary to intrinsic apoptosis (Figure 3D). Moreover, it has been shown that Smac mimetics result in ripoptosome-caspase-8-mediated NLRP3-inflammasome activation (Lawlor et al., 2015). Nonetheless, how caspase-8 activates NLRP3-caspase-1 in this context remains unknown. To determine which signaling step of the MOMP-ripoptosome-caspase-8 cascade triggers NLRP3, we studied NLRP3 activation in *Casp8*$^{-/-}$/*Ripk3*$^{-/-}$ and *Ripk3*$^{-/-}$ macrophages (Figures 7A and 7B). Cells were primed with LPS and stimulated with nigericin, Vio A, and birinapant in the presence or absence of MCC950, a specific NLRP3 inhibitor (Coll et al., 2015). As expected, nigericin-mediated caspase-1 activation was completely abrogated in the presence of MCC950 in all of the genotypes (Figures 7A and 7B) (Coll et al., 2015). In addition to IL-1β maturation, MCC950 inhibited LDH release after

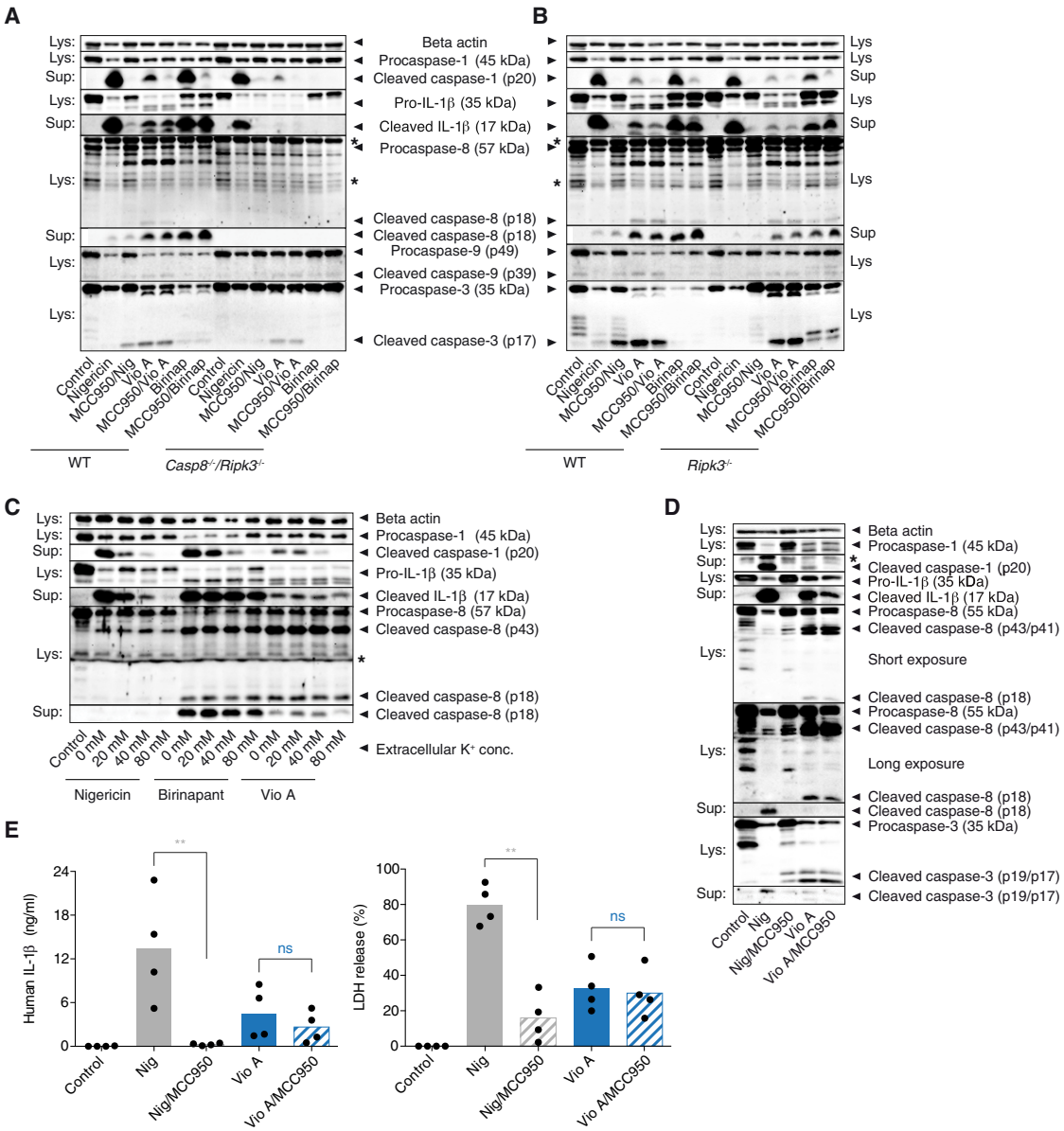

Figure 7. Intrinsic Apoptosis Results in Ripoptosome-Caspase-8-Dependent and -Independent NLRP3-Caspase-1 Activation

(A and B) Immunoblot of (A) WT and *Casp8*$^{-/-}$/*Ripk3*$^{-/-}$ or (B) WT and *Ripk3*$^{-/-}$ BMDMs primed with LPS (1,000 ng/mL) for 4 hr and stimulated with nigericin, birinapant, and Vio A in the presence or absence of MCC950 (added in the last hour of priming).

(C) WT BMDMs were primed with LPS (200 ng/mL) for 4 hr, followed by the addition of indicated concentrations of K^+ in the medium in the last 15 min of priming. Samples were stimulated with nigericin, birinapant, and Vio A (20 μM) and analyzed by immunoblot after 8 hr.

(D and E) Primary human monocytes were primed with Pam3CSK4 for 4 hr and followed by stimulation of nigericin and Vio A in the absence and presence of MCC950. MCC950 was added in the last hour of priming. After 6 hr, samples were analyzed for (D) immunoblot and (E) IL-1β and LDH release.

Data are representative of (A and B) two, (C and D) three and (E) four independent experiments/donors. *Non-specific cross-reactivity of the antibody.

See also Figure S7.

nigericin treatment (Figures S7A and S7B). In line with previous work (Lawlor et al., 2015), the Smac mimetic birinapant resulted in NLRP3-dependent caspase-1 processing that occurred downstream of ripoptosome/caspase-8-activation, and *Ripk3* deficiency on its own led to reduced caspase-8 and caspase-1 activation. However, birinapant-mediated LDH release proceeded independently of NLRP3 (Figures S7A and S7B). Similarly, Vio A-dependent caspase-1 activation was fully NLRP3 dependent. While the majority of this inflammasome response occurred downstream of ripoptosome/caspase-8, we also observed a small-proportion caspase-8-independent NLRP3 activation (Figure 7A).

To further characterize the observed phenomenon of caspase-8-dependent NLRP3 activation, we used a hyperkalemic

extracellular buffer, which inhibits NLRP3 inflammasome activation in the context of membrane perturbation (Franchi et al., 2007; Pétrilli et al., 2007). In keeping with previously published studies, elevated potassium levels inhibited caspase-1 maturation and IL-1β release downstream of the NLRP3 activator nigericin (Figure 7C). At the same time, hyperkalemic extracellular conditions completely abrogated caspase-1 activation upon birinapant and Vio A treatment. In contrast, increased extracellular potassium levels had no impact on caspase-8 processing and only a slight effect on IL-1β release after birinapant and Vio A stimulation. Next, to determine the ability of Vio A to induce MOMP in other cell types, we used murine embryonic fibroblasts (MEFs). Similar to macrophages, MEFs also require two triggers for the induction of MOMP (White et al., 2014). In line with our previous results, Vio A also induced MOMP in MEFs cells, albeit with somewhat delayed kinetics, similar to the results obtained in SVECs (Figure S7C).

Furthermore, to assess the bioactivity of Vio A in human cells and compare the observations with the murine system, primary monocytes were isolated from human PBMCs. To circumvent alternative inflammasome activation (Gaidt et al., 2016), cells were primed with Pam3CSK4 and stimulated with nigericin and Vio A in the absence or presence of the NLRP3 inhibitor (MCC950) (Figures 7D and 7E). As expected, nigericin led to IL-1β and LDH secretion (Gaidt et al., 2017) (Figure 7E), which correlated with the release of cleaved caspase-1 into the supernatant (Figure 7D). Moreover, this release of mature IL-1β and caspase-1 and nigericin-induced LDH release was completely blocked by the addition of MCC950 (Figure 7E). Similar to BMDMs, Vio A also resulted in IL-1β and LDH release in human monocytes. However, unlike nigericin, IL-1β and LDH release by Vio A was largely independent of NLRP3 inhibition, and this IL-1β release correlated with caspase-8 activation (Figure 7D). Furthermore, MCC950 blocked the cleavage of Vio A-induced caspase-1 in monocytes, while the activity of caspase-8 and caspase-3 was largely unaffected (Figure 7D). In line with our findings in murine cells, this inhibition of caspase-1 activation also had no substantial effect on IL-1β release (Figures 7A and 7D).

In summary, our data indicate that vioprolide-induced ripoptosome/caspase-8 activation constitutes the prime mechanism of IL-1β maturation in the context of MOMP. Moreover, in addition to this functionality, caspase-8 triggers a lytic cell death that results in K^+ efflux and thereby secondary activation of the NLRP3 inflammasome. However, this mechanism has only a subordinate role in the observed IL-1β maturation (Figure S7D).

DISCUSSION

Here, we formally define a signaling route that connects intrinsic apoptosis to the activation of IL-1β, a gatekeeper cytokine of inflammation. Validating hits from a small molecule screen aimed at identifying previously uncharacterized regulators of inflammasome activation, we identified vioprolides as a class of compounds that can trigger IL-1β maturation in macrophages. This functionality turned out to be largely independent of inflammasome activation. Instead, vioprolide-dependent IL-1β maturation was found to be connected to its capacity to trigger intrinsic apoptosis. As such, vioprolides initiate MOMP in a BAX/BAK-dependent manner via two distinct functionalities: on the one hand, they act as translation inhibitors, which result in a decrease in MCL-1 levels, a pivotal pro-survival BCL2 family protein; on the other hand, they confer a second signal through BCL2 inhibition to initiate BAX/BAK-dependent MOMP. In keeping with this mode of action, we could mimic all vioprolide-dependent effects by treating macrophages with a combination of a translational inhibitor to decrease MCL-1 levels and the compound ABT-737 to trigger BAX/BAK activation. While the induction of MOMP results in the activation of intrinsic apoptosis via caspase-9, it also initiates in IAP depletion. Consequently, depletion of IAPs leads to a caspase-8-containing ripoptosome complex that directly matures IL-1β. Caspase-8 activity also amplifies intrinsic apoptosis, most probably via BID cleavage. Of note, at later time points, vioprolides also induced cell death and IL-1β release independently of NLRP3 in $Bax^{-/-}/Bak1^{-/-}$ cells (data not shown). Nevertheless, this BAX/BAK-independent cell death also resulted in IAP depletion and subsequent caspase-8-dependent IL-1β maturation. As a consequence of these processes, plasma membrane integrity is breached, additionally resulting in caspase-8 dependent and -independent K^+ efflux, leading to NLRP3 activation. However, it should be noted that under these conditions, NLRP3 activity only plays a minor role in IL-1β maturation and cell death. In summary, using genetic and biochemical tools, we formally establish MOMP as a pro-inflammatory process in macrophages, with the ripoptosome complex functioning as its central molecular switch.

The Inflammasome Plays a Subordinate Role in MOMP-Triggered Inflammation

While previous studies have implied mitochondrial perturbation in the context of inflammasome-driven IL-1β maturation, these reports established a connection between classical NLRP3 stimuli and MOMP downstream of K^+ efflux (Iyer et al., 2013; Shimada et al., 2012). Using genetic loss-of-functions approaches, we can clearly show that MOMP is dispensable for this route of NLRP3 activation. Nevertheless, dissecting intrinsic apoptosis induction upstream of MOMP, we can establish MOMP as a distinctive signal that leads to the release of bioactive IL-1β, although in a different context. In fact, in this response pathway it is specifically the activity of the ripoptosome/caspase-8 complex and not of the NLRP3 inflammasome that governs IL-1β maturation. This is intriguing in that NLRP3 activity is tightly connected to cell damage, sensing K^+ efflux as a proxy of membrane integrity (Gaidt and Hornung, 2018). We also observe K^+ efflux-dependent NLRP3 inflammasome activation as a consequence of MOMP, but this is a late event that is governed by the loss of membrane integrity downstream of apoptotic caspase activation (McCarthy and Cotter, 1997). In agreement with this late engagement of the inflammasome pathway, GSDMD deficiency could not rescue the loss of membrane integrity that was observed downstream of MOMP. Given that the kinetics of inflammasome activation normally supersede apoptotic signaling cascades in regard to determining the cell fate, these results underscore the unique functionality of apoptosis in maintaining membrane integrity.

Intrinsic Apoptosis Is Not a Silent Cell Death Program in Myeloid Cells

In light of the important functions of apoptosis during development and tissue homeostasis, this programmed cell death has been long considered to be immunologically silent. This is achieved by complex communication between apoptotic cells and surrounding phagocytes that leads to rapid uptake and clearance of the apoptotic content. During this process, the plasma membrane is considered to be intact, enabling sequestration of putative DAMP molecules within apoptotic bodies to prevent inflammation (Poon et al., 2014). In fact, apoptotic pathways display even anti-inflammatory (inflammation-suppressive) features: efferocytosis is known to induce an anti-inflammatory state in the respective phagocyte (Poon et al., 2014), whereas the apoptotic death actively avoids the initiation of cell-intrinsic pro-inflammatory program (e.g., NF-κB, cGAS-STING [stimulator of interferon genes protein]) activation during perturbed mitochondrial integrity (Giampazolias et al., 2017; Rongvaux et al., 2014; White et al., 2014), or NF-κB activation by several death ligands, including TNF-related apoptosis-inducing ligand (TRAIL), FAS, or TNF (Park et al., 2005).

Nonetheless, a number of reports have indicated apoptosis as a potent mediator of inflammation in *in vitro* as well as *in vivo* settings (Bossaller et al., 2012; Faouzi et al., 2001). Although the detailed molecular mechanisms of apoptosis-mediated inflammation have remained elusive, the present study provides conclusive evidence that intrinsic apoptosis triggers pro-inflammatory signaling through the maturation of IL-1β. Although initially guided by the characterization of vioprolides, which can trigger intrinsic apoptosis in macrophages via a 2-fold functionality, the inflammatory consequences of vioprolide-mediated apoptosis are generally applicable to apoptotic cell death programs. As such, treating macrophages with cycloheximide and ABT-737 resulted in the same response pattern. Furthermore, it is presumable that cytokine release is not the only pro-inflammatory aspect of apoptotic cell death. It has been shown that other cell types, such as epithelial cells or keratinocytes, are capable of ripoptosome formation (Feoktistova et al., 2011; Tenev et al., 2011). Given that these cells do not express IL-1β, it will be of interest to determine whether and how the MOMP-apoptotic factors-IAP depletion-ripotosome-caspase-8 pathway triggers inflammation here.

The Ripoptosome Functions as an Innate Sensor

IL-1β maturation by inflammasomes is an important aspect of the antimicrobial immune defense, with inflammasome receptors serving as "non-self-recognition units." While certain inflammasome receptors do not participate in direct pattern recognition, their domain architecture and signaling cascades are shared with bona fide pattern recognition receptors (PRRs). An intriguing finding of our work is that there is no PRR or PRR-like molecule required for IL-1β maturation during intrinsic apoptosis. Instead, it is the ripoptosome complex that functions as an indirect sensor of organelle integrity (MOMP), with IAP depletion as its activating signal. Of note, IAP depletion coinciding with caspase-8 activation was not only seen for the early BAX/BAK-dependent pathway of vioprolide-dependent IL-1β maturation but also observed for the late, BAX/BAK-independent pathway. These observations further strengthen the role of the ripoptosome/caspase-8 complex in damage sensing. This mode of action is in keeping with the concept of effector-triggered immunity (ETI), in which cells identify pathogen-driven disturbances rather than pathogen-derived molecular patterns (Stuart et al., 2013). From the host perspective, this mode of recognition bears the advantage of being independent of a specific microbial pattern, which may evade recognition under selection pressure. In this context, it is intriguing that IAP molecules are involved in two distinct signaling capacities, both serving the induction of pro-inflammatory responses. On the one hand, IAP molecules play crucial roles in propagating pro-inflammatory signal transduction cascades downstream of PRR and cytokine receptors (Darding and Meier, 2012). On the other hand, their presence is critically required to prevent the formation of a ripoptosome/caspase-8 complex that can mature the highly pro-inflammatory cytokine IL-1β. These characteristics enable IAP molecules to serve as the rheostat of two independent pro-inflammatory signaling cascades.

While our study does not formally establish the ripoptosome as a pathogen-driven ETI sensor, it is noteworthy that ripoptosome-dependent ETI seems not to be limited to MOMP-mediated activation. To this end, the *Yersinia pestis* effector YopJ has been reported to induce caspase-8-dependent IL-1β maturation in a BAX/BAK-independent fashion (Weng et al., 2014; Zheng et al., 2012). Formally establishing the ripoptosome as an ETI sensor under these pathogenic settings could provide further insights into IL-1β maturation pathways and ETI in the mammalian system in general.

STAR★METHODS

Detailed methods are provided in the online version of this paper and include the following:

- KEY RESOURCES TABLE
- CONTACT FOR REAGENT AND RESOURCE SHARING
- EXPERIMENTAL MODEL AND SUBJECT DETAILS
  - Mice
  - Preparation of murine bone marrow derived macrophages (BMDMs)
  - Isolation of human primary cells
  - Primary cell culture
  - Cell lines
- METHODS DETAILS
  - Cell stimulation
  - Immunoblotting, LDH and ELISA assay
  - Quantitative PCR
  - Cytoplasmic extraction of BMDMs
  - DNA laddering assay
  - Plasmid preparation for hemoglobin subunit beta (HBB)
  - Human *in vitro* translation extract
  - *In vitro* transcription
  - *In vitro* translation
  - Mito-priming Assay
- QUANTIFICATION AND STATISTICAL ANALYSIS
  - Statistical analysis
- DATA AND SOFTWARE AVAILABILITY

SUPPLEMENTAL INFORMATION

Supplemental Information includes seven figures and can be found with this article online at https://doi.org/10.1016/j.celrep.2018.10.087.

ACKNOWLEDGMENTS

We kindly thank Maximillian Rothe (Institute of Innate Immunity, University of Bonn) and Christina Wallerath (Institute of Clinical Chemistry and Clinical Pharmacology, University of Bonn) for great technical support, Dr. Vishva Dixit for *Nlrp3* and *Pycard*-deficient mice (Genentech, USA), Dr. James Vince (Walter and Eliza Hall Institute of Medical Research [WEHI], Australia) for *Bax/Bak1*-deficient bone marrow cells, and Dr. Richard A. Flavell (Yale University, USA) for providing *Casp1/11*-deficient mice. *Casp8*$^{-/-}$*/Ripk3*$^{-/-}$ and *Ripk3*$^{-/-}$ were a gift from Dr. Egil Lien (University of Massachusetts Medical School, USA). This work was supported by a grant from the DZIF 09.804 (German Center for Infection Research) to V.H.

AUTHOR CONTRIBUTIONS

D.C. performed most of the experiments. E.B. assisted in the majority of the experiments. J.M.S. and H.K. assisted in the experiment with Figures S4C and S4D. F.J.B. and S.W.G.T. performed the mito-priming experiments. J.H. and R.M. provided the screening library and Vio A–D. P.B. provided *Gsdmd*-deficient cells. D.C., E.B., M.M.G., and V.H. planned the experiments, and D.C., E.B., and V.H. wrote the manuscript with input from all of the authors. V.H. conceived and supervised the study.

DECLARATION OF INTERESTS

V.H. serves on the scientific advisory board of Inflazome, Ltd.

Received: March 23, 2018
Revised: August 14, 2018
Accepted: October 24, 2018
Published: November 27, 2018

REFERENCES

Adams, K.W., and Cooper, G.M. (2007). Rapid turnover of mcl-1 couples translation to cell survival and apoptosis. J. Biol. Chem. *282*, 6192–6200.

Afonina, I.S., Müller, C., Martin, S.J., and Beyaert, R. (2015). Proteolytic processing of interleukin-1 family cytokines: variations on a common theme. Immunity *42*, 991–1004.

Allam, R., Lawlor, K.E., Yu, E.C., Mildenhall, A.L., Moujalled, D.M., Lewis, R.S., Ke, F., Mason, K.D., White, M.J., Stacey, K.J., et al. (2014). Mitochondrial apoptosis is dispensable for NLRP3 inflammasome activation but non-apoptotic caspase-8 is required for inflammasome priming. EMBO Rep. *15*, 982–990.

Antonopoulos, C., El Sanadi, C., Kaiser, W.J., Mocarski, E.S., and Dubyak, G.R. (2013). Proapoptotic chemotherapeutic drugs induce noncanonical processing and release of IL-1β via caspase-8 in dendritic cells. J. Immunol. *191*, 4789–4803.

Antonopoulos, C., Russo, H.M., El Sanadi, C., Martin, B.N., Li, X., Kaiser, W.J., Mocarski, E.S., and Dubyak, G.R. (2015). Caspase-8 as an effector and regulator of NLRP3 inflammasome signaling. J. Biol. Chem. *290*, 20167–20184.

Austin, M., and Cook, S.J. (2005). Increased expression of Mcl-1 is required for protection against serum starvation in phosphatase and tensin homologue on chromosome 10 null mouse embryonic fibroblasts, but repression of Bim is favored in human glioblastomas. J. Biol. Chem. *280*, 33280–33288.

Bauernfeind, F.G., Horvath, G., Stutz, A., Alnemri, E.S., MacDonald, K., Speert, D., Fernandes-Alnemri, T., Wu, J., Monks, B.G., Fitzgerald, K.A., et al. (2009). Cutting edge: NF-kappaB activating pattern recognition and cytokine receptors license NLRP3 inflammasome activation by regulating NLRP3 expression. J. Immunol. *183*, 787–791.

Bieging, K.T., Amick, A.C., and Longnecker, R. (2009). Epstein-Barr virus LMP2A bypasses p53 inactivation in a MYC model of lymphomagenesis. Proc. Natl. Acad. Sci. USA *106*, 17945–17950.

Bollati-Fogolin, M., and Müller, W. (2008). Interferon type i supporting compounds. Google patent filed October 12, 2006, and published June 19, 2008.

Bossaller, L., Chiang, P.I., Schmidt-Lauber, C., Ganesan, S., Kaiser, W.J., Rathinam, V.A., Mocarski, E.S., Subramanian, D., Green, D.R., Silverman, N., et al. (2012). Cutting edge: FAS (CD95) mediates noncanonical IL-1β and IL-18 maturation via caspase-8 in an RIP3-independent manner. J. Immunol. *189*, 5508–5512.

Broz, P., and Dixit, V.M. (2016). Inflammasomes: mechanism of assembly, regulation and signalling. Nat. Rev. Immunol. *16*, 407–420.

Coll, R.C., Robertson, A.A., Chae, J.J., Higgins, S.C., Muñoz-Planillo, R., Inserra, M.C., Vetter, I., Dungan, L.S., Monks, B.G., Stutz, A., et al. (2015). A small-molecule inhibitor of the NLRP3 inflammasome for the treatment of inflammatory diseases. Nat. Med. *21*, 248–255.

Conos, S.A., Lawlor, K.E., Vaux, D.L., Vince, J.E., and Lindqvist, L.M. (2016). Cell death is not essential for caspase-1-mediated interleukin-1β activation and secretion. Cell Death Differ. *23*, 1827–1838.

Darding, M., and Meier, P. (2012). IAPs: guardians of RIPK1. Cell Death Differ. *19*, 58–66.

Dillon, C.P., Weinlich, R., Rodriguez, D.A., Cripps, J.G., Quarato, G., Gurung, P., Verbist, K.C., Brewer, T.L., Llambi, F., Gong, Y.N., et al. (2014). RIPK1 blocks early postnatal lethality mediated by caspase-8 and RIPK3. Cell *157*, 1189–1202.

Dinarello, C.A. (2011). A clinical perspective of IL-1β as the gatekeeper of inflammation. Eur. J. Immunol. *41*, 1203–1217.

Dzhagalov, I., St John, A., and He, Y.W. (2007). The antiapoptotic protein Mcl-1 is essential for the survival of neutrophils but not macrophages. Blood *109*, 1620–1626.

Elmore, S. (2007). Apoptosis: a review of programmed cell death. Toxicol. Pathol. *35*, 495–516.

England, H., Summersgill, H.R., Edye, M.E., Rothwell, N.J., and Brough, D. (2014). Release of interleukin-1α or interleukin-1β depends on mechanism of cell death. J. Biol. Chem. *289*, 15942–15950.

Evavold, C.L., Ruan, J., Tan, Y., Xia, S., Wu, H., and Kagan, J.C. (2018). The pore-forming protein gasdermin D regulates interleukin-1 secretions from living macrophages. Immunity *48*, 35–44.e6.

Faouzi, S., Burckhardt, B.E., Hanson, J.C., Campe, C.B., Schrum, L.W., Rippe, R.A., and Maher, J.J. (2001). Anti-Fas induces hepatic chemokines and promotes inflammation by an NF-kappa B-independent, caspase-3-dependent pathway. J. Biol. Chem. *276*, 49077–49082.

Feoktistova, M., Geserick, P., Kellert, B., Dimitrova, D.P., Langlais, C., Hupe, M., Cain, K., MacFarlane, M., Häcker, G., and Leverkus, M. (2011). cIAPs block ripoptosome formation, a RIP1/caspase-8 containing intracellular cell death complex differentially regulated by cFLIP isoforms. Mol. Cell *43*, 449–463.

Franchi, L., Kanneganti, T.D., Dubyak, G.R., and Núñez, G. (2007). Differential requirement of P2X7 receptor and intracellular K+ for caspase-1 activation induced by intracellular and extracellular bacteria. J. Biol. Chem. *282*, 18810–18818.

Gaidt, M.M., and Hornung, V. (2018). The NLRP3 inflammasome renders cell death pro-inflammatory. J. Mol. Biol. *430*, 133–141.

Gaidt, M.M., Ebert, T.S., Chauhan, D., Schmidt, T., Schmid-Burgk, J.L., Rapino, F., Robertson, A.A., Cooper, M.A., Graf, T., and Hornung, V. (2016). Human monocytes engage an alternative inflammasome pathway. Immunity *44*, 833–846.

Gaidt, M.M., Ebert, T.S., Chauhan, D., Ramshorn, K., Pinci, F., Zuber, S., O'Duill, F., Schmid-Burgk, J.L., Hoss, F., Buhmann, R., et al. (2017). The DNA inflammasome in human myeloid cells is initiated by a STING-cell death program upstream of NLRP3. Cell *171*, 1110–1124.e18.

Giampazolias, E., Zunino, B., Dhayade, S., Bock, F., Cloix, C., Cao, K., Roca, A., Lopez, J., Ichim, G., Proïcs, E., et al. (2017). Mitochondrial permeabilization

engages NF-κB-dependent anti-tumour activity under caspase deficiency. Nat. Cell Biol. *19*, 1116–1129.

Herrmann, J., Fayad, A.A., and Müller, R. (2017). Natural products from myxobacteria: novel metabolites and bioactivities. Nat. Prod. Rep. *34*, 135–160.

Iyer, S.S., He, Q., Janczy, J.R., Elliott, E.I., Zhong, Z., Olivier, A.K., Sadler, J.J., Knepper-Adrian, V., Han, R., Qiao, L., et al. (2013). Mitochondrial cardiolipin is required for Nlrp3 inflammasome activation. Immunity *39*, 311–323.

Jakobs, C., Bartok, E., Kubarenko, A., Bauernfeind, F., and Hornung, V. (2013). Immunoblotting for active caspase-1. Methods Mol. Biol. *1040*, 103–115.

Juliana, C., Fernandes-Alnemri, T., Kang, S., Farias, A., Qin, F., and Alnemri, E.S. (2012). Non-transcriptional priming and deubiquitination regulate NLRP3 inflammasome activation. J. Biol. Chem. *287*, 36617–36622.

Kaiser, W.J., Upton, J.W., Long, A.B., Livingston-Rosanoff, D., Daley-Bauer, L.P., Hakem, R., Caspary, T., and Mocarski, E.S. (2011). RIP3 mediates the embryonic lethality of caspase-8-deficient mice. Nature *471*, 368–372.

Kayagaki, N., Stowe, I.B., Lee, B.L., O'Rourke, K., Anderson, K., Warming, S., Cuellar, T., Haley, B., Roose-Girma, M., Phung, Q.T., et al. (2015). Caspase-11 cleaves gasdermin D for non-canonical inflammasome signalling. Nature *526*, 666–671.

Knittel, G., Liedgens, P., Korovkina, D., Seeger, J.M., Al-Baldawi, Y., Al-Maarri, M., Fritz, C., Vlantis, K., Bezhanova, S., Scheel, A.H., et al.; German International Cancer Genome Consortium Molecular Mechanisms in Malignant Lymphoma by Sequencing Project Consortium (2016). B-cell-specific conditional expression of Myd88p.L252P leads to the development of diffuse large B-cell lymphoma in mice. Blood *127*, 2732–2741.

Kralj, M., Husnjak, K., Körbler, T., and Pavelić, J. (2003). Endogenous p21WAF1/CIP1 status predicts the response of human tumor cells to wild-type p53 and p21WAF1/CIP1 overexpression. Cancer Gene Ther. *10*, 457–467.

Kuida, K., Lippke, J.A., Ku, G., Harding, M.W., Livingston, D.J., Su, M.S., and Flavell, R.A. (1995). Altered cytokine export and apoptosis in mice deficient in interleukin-1 beta converting enzyme. Science *267*, 2000–2003.

Lawlor, K.E., Khan, N., Mildenhall, A., Gerlic, M., Croker, B.A., D'Cruz, A.A., Hall, C., Kaur Spall, S., Anderton, H., Masters, S.L., et al. (2015). RIPK3 promotes cell death and NLRP3 inflammasome activation in the absence of MLKL. Nat. Commun. *6*, 6282.

Liu, X., Zhang, Z., Ruan, J., Pan, Y., Magupalli, V.G., Wu, H., and Lieberman, J. (2016). Inflammasome-activated gasdermin D causes pyroptosis by forming membrane pores. Nature *535*, 153–158.

Lopez, J., Bessou, M., Riley, J.S., Giampazolias, E., Todt, F., Rochegüe, T., Oberst, A., Green, D.R., Edlich, F., Ichim, G., and Tait, S.W. (2016). Mito-priming as a method to engineer Bcl-2 addiction. Nat. Commun. *7*, 10538.

Maelfait, J., Vercammen, E., Janssens, S., Schotte, P., Haegman, M., Magez, S., and Beyaert, R. (2008). Stimulation of Toll-like receptor 3 and 4 induces interleukin-1beta maturation by caspase-8. J. Exp. Med. *205*, 1967–1973.

Mariathasan, S., Newton, K., Monack, D.M., Vucic, D., French, D.M., Lee, W.P., Roose-Girma, M., Erickson, S., and Dixit, V.M. (2004). Differential activation of the inflammasome by caspase-1 adaptors ASC and Ipaf. Nature *430*, 213–218.

Mariathasan, S., Weiss, D.S., Newton, K., McBride, J., O'Rourke, K., Roose-Girma, M., Lee, W.P., Weinrauch, Y., Monack, D.M., and Dixit, V.M. (2006). Cryopyrin activates the inflammasome in response to toxins and ATP. Nature *440*, 228–232.

Masters, S.L., Simon, A., Aksentijevich, I., and Kastner, D.L. (2009). Horror autoinflammaticus: the molecular pathophysiology of autoinflammatory disease (*). Annu. Rev. Immunol. *27*, 621–668.

Matheisl, S., Berninghausen, O., Becker, T., and Beckmann, R. (2015). Structure of a human translation termination complex. Nucleic Acids Res. *43*, 8615–8626.

McCarthy, J.V., and Cotter, T.G. (1997). Cell shrinkage and apoptosis: a role for potassium and sodium ion efflux. Cell Death Differ. *4*, 756–770.

Newton, K., Sun, X., and Dixit, V.M. (2004). Kinase RIP3 is dispensable for normal NF-kappa Bs, signaling by the B-cell and T-cell receptors, tumor necrosis factor receptor 1, and Toll-like receptors 2 and 4. Mol. Cell. Biol. *24*, 1464–1469.

Oberst, A., Dillon, C.P., Weinlich, R., McCormick, L.L., Fitzgerald, P., Pop, C., Hakem, R., Salvesen, G.S., and Green, D.R. (2011). Catalytic activity of the caspase-8-FLIP(L) complex inhibits RIPK3-dependent necrosis. Nature *471*, 363–367.

Oltersdorf, T., Elmore, S.W., Shoemaker, A.R., Armstrong, R.C., Augeri, D.J., Belli, B.A., Bruncko, M., Deckwerth, T.L., Dinges, J., Hajduk, P.J., et al. (2005). An inhibitor of Bcl-2 family proteins induces regression of solid tumours. Nature *435*, 677–681.

Park, S.M., Schickel, R., and Peter, M.E. (2005). Nonapoptotic functions of FADD-binding death receptors and their signaling molecules. Curr. Opin. Cell Biol. *17*, 610–616.

Park, S., Juliana, C., Hong, S., Datta, P., Hwang, I., Fernandes-Alnemri, T., Yu, J.W., and Alnemri, E.S. (2013). The mitochondrial antiviral protein MAVS associates with NLRP3 and regulates its inflammasome activity. J. Immunol. *191*, 4358–4366.

Pétrilli, V., Papin, S., Dostert, C., Mayor, A., Martinon, F., and Tschopp, J. (2007). Activation of the NALP3 inflammasome is triggered by low intracellular potassium concentration. Cell Death Differ. *14*, 1583–1589.

Poon, I.K., Lucas, C.D., Rossi, A.G., and Ravichandran, K.S. (2014). Apoptotic cell clearance: basic biology and therapeutic potential. Nat. Rev. Immunol. *14*, 166–180.

Rongvaux, A., Jackson, R., Harman, C.C., Li, T., West, A.P., de Zoete, M.R., Wu, Y., Yordy, B., Lakhani, S.A., Kuan, C.Y., et al. (2014). Apoptotic caspases prevent the induction of type I interferons by mitochondrial DNA. Cell *159*, 1563–1577.

Schneider, K.S., Groß, C.J., Dreier, R.F., Saller, B.S., Mishra, R., Gorka, O., Heilig, R., Meunier, E., Dick, M.S., Ćiković, T., et al. (2017). The inflammasome drives GSDMD-independent secondary pyroptosis and IL-1 release in the absence of caspase-1 protease activity. Cell Rep. *21*, 3846–3859.

Schummer, D., Höfle, G., Forche, E., Reichenbach, H., Wray, V., and Domke, T. (1996). Antibiotics from gliding bacteria, LXXVI. Vioprolides: new antifungal and cytotoxic peptolides from Cystobacter violaceus. Liebigs Ann. *1996*, 971–978.

Shi, J., Zhao, Y., Wang, K., Shi, X., Wang, Y., Huang, H., Zhuang, Y., Cai, T., Wang, F., and Shao, F. (2015). Cleavage of GSDMD by inflammatory caspases determines pyroptotic cell death. Nature *526*, 660–665.

Shimada, K., Crother, T.R., Karlin, J., Dagvadorj, J., Chiba, N., Chen, S., Ramanujan, V.K., Wolf, A.J., Vergnes, L., Ojcius, D.M., et al. (2012). Oxidized mitochondrial DNA activates the NLRP3 inflammasome during apoptosis. Immunity *36*, 401–414.

Stuart, L.M., Paquette, N., and Boyer, L. (2013). Effector-triggered versus pattern-triggered immunity: how animals sense pathogens. Nat. Rev. Immunol. *13*, 199–206.

Surup, F., Chauhan, D., Niggemann, J., Bartok, E., Herrmann, J., Keck, M., Zander, W., Stadler, M., Hornung, V., and Muller, R. (2018). Activation of the NLRP3 inflammasome by hyaboron, a new asymmetric boron-containing macrodiolide from the myxobacterium Hyalangium minutum. ACS Chem Biol *13*, 2981–2988.

Tenev, T., Bianchi, K., Darding, M., Broemer, M., Langlais, C., Wallberg, F., Zachariou, A., Lopez, J., MacFarlane, M., Cain, K., and Meier, P. (2011). The ripoptosome, a signaling platform that assembles in response to genotoxic stress and loss of IAPs. Mol. Cell *43*, 432–448.

Vince, J.E., Wong, W.W., Gentle, I., Lawlor, K.E., Allam, R., O'Reilly, L., Mason, K., Gross, O., Ma, S., Guarda, G., et al. (2012). Inhibitor of apoptosis proteins limit RIP3 kinase-dependent interleukin-1 activation. Immunity *36*, 215–227.

Weissman, K.J., and Müller, R. (2010). Myxobacterial secondary metabolites: bioactivities and modes-of-action. Nat. Prod. Rep. *27*, 1276–1295.

Weng, D., Marty-Roix, R., Ganesan, S., Proulx, M.K., Vladimer, G.I., Kaiser, W.J., Mocarski, E.S., Pouliot, K., Chan, F.K., Kelliher, M.A., et al. (2014).

Caspase-8 and RIP kinases regulate bacteria-induced innate immune responses and cell death. Proc. Natl. Acad. Sci. USA *111*, 7391–7396.

White, M.J., McArthur, K., Metcalf, D., Lane, R.M., Cambier, J.C., Herold, M.J., van Delft, M.F., Bedoui, S., Lessene, G., Ritchie, M.E., et al. (2014). Apoptotic caspases suppress mtDNA-induced STING-mediated type I IFN production. Cell *159*, 1549–1562.

Yan, F., Auerbach, D., Chai, Y., Keller, L., Tu, Q., Huttel, S., Glemser, A., Grab, H.A., Bach, T., Zhang, Y., and Muller, R. (2018). Biosynthesis and heterologous production of vioprolides: rational biosynthetic engineering and unprecedented 4-methylazetidinecarboxylic acid formation. Angew. Chem. Int. Ed. Engl. *57*, 8754–8759.

Youle, R.J., and Strasser, A. (2008). The BCL-2 protein family: opposing activities that mediate cell death. Nat. Rev. Mol. Cell Biol. *9*, 47–59.

Zheng, Y., Lilo, S., Mena, P., and Bliska, J.B. (2012). YopJ-induced caspase-1 activation in Yersinia-infected macrophages: independent of apoptosis, linked to necrosis, dispensable for innate host defense. PLoS One *7*, e36019.

STAR★METHODS

KEY RESOURCES TABLE

REAGENT or RESOURCE	SOURCE	IDENTIFIER
Antibodies		
BAX	Cell Signaling Technology	Cat#2772
BAK (Polyclonal rabbit)	BD Biosciences	Cat#556396
BCL2 (Purified mouse) Clone 7/Bcl-2	BD Biosciences	Cat#610539
Beta actin antibody (C4)	Santa Cruz Biotechnology	Cat#Sc-47778
BID (Human/Mouse)	R&D systems	Cat#AF860
Caspase-1 (p20) (human), mAb (Bally-1)	Adipogen International	Cat#AG-20B-0048-C100
Caspase-1 (p20) (mouse), mAb (Casper-1)	Adipogen International	Cat#AG-20B-0042-C100
Caspase-3	Cell Signaling Technology	Cat#9662
Caspase-8 (Asp 387) (Cleaved-Mouse specific)	Cell Signaling Technology	Cat#9429
Caspase-8 (Full length-Mouse specific)	Cell Signaling Technology	Cat#4927
Caspase-8 (human) monoclonal antibody (12F5)	Enzo Life Sciences	Cat#ALX-804-242-C100
Caspase-9 (Mouse specific)	Cell Signaling Technology	Cat#9504
cIAP1 monoclonal antibody (1E1-1-10)	Enzo Life Sciences	Cat#ALX-803-335-C100
cIAP2	Merck Millipore	Cat#AB3615
COXIV	Cell Signaling Technology	Cat#4844
Cytochrome C	Santa Cruz Biotechnology	Cat#Sc-7159
donkey anti-goat IgG-HRP	Santa Cruz Biotechnology	Cat#sc-2020
goat anti-mouse IgG-HRP	Santa Cruz Biotechnology	Cat#sc-2005
goat anti-rabbit IgG-HRP	Santa Cruz Biotechnology	Cat#sc-2004
goat anti-rat IgG-HRP	Santa Cruz Biotechnology	Cat#sc-2032
HA-antibody (Produced in Rabbit)	Sigma Aldrich	Cat#H6908
Human IL-1β/IL-1F2 Antibody	R&D systems	Cat#AF-201-NA
Mcl-1 (D35A5) Rabbit	Cell Signaling Technology	Cat#5453
Mouse IL-1 beta /IL-1F2 Antibody	R&D systems	Cat#AF-401-NA
Smac/DIABLO (mouse) monoclonal antibody (9H10)	Enzo Life Sciences	Cat#ALX-804-366-C100
XIAP	Cell Signaling Technology	Cat#2042
Chemicals, Peptides, and Recombinant Proteins		
A-1155463 (BCL-X_L inhibitor)	AdooQ Bioscience	Cat#A16112
ABT-199	AdooQ Bioscience	Cat#A12500-50
ABT-737	AdooQ Bioscience	Cat# A10255-100
Actinomycin D	AdooQ Bioscience	Cat#A13239-10
Birinapant	BioVision	Cat#2597-1
Cycloheximide	Carl Roth	Cat#8682.3
Lipofectamine 2000 Transfection Reagent	Thermo Fisher Scientific	Cat#11668019
LPS-EB Ultrapure	InvivoGen	Cat#tlrl-3pelps
MCC950 (CP-456773)	Tocris Bioscience	Cat# 5479
MG-132	Selleck Chemicals	Cat# S2619
Nigericin sodium salt	Sigma-Aldrich	Cat#N7143-10MG
Pam3CSK4	InvivoGen	Cat#tlrl-pms
R848 (Resiquimod)	InvivoGen	Cat# tlrl-r848
S63845 (MCL-1 inhibitor)	APExBIO	Cat#A8737
Staurosporine (CAS 62996-74-1)	Santa Cruz Biotechnology	Cat#sc-3510A
SYTOX ™ Green Nucleic Acid Stain	Thermo Fisher Scientific	Cat#S7020

(*Continued on next page*)

Continued

REAGENT or RESOURCE	SOURCE	IDENTIFIER
Critical Commercial Assays		
CD14 MicroBeads, Human	Miltenyi Biotec	Cat#130-050-201
Human IL-1β ELISA Set II	BD Biosciences	Cat#557953
Pierce LDH Cytotoxicity Assay Kit	Thermo Fisher Scientific	Cat#88954
Mouse IL-1β ELISA Set	BD Biosciences	Cat#559603
Pierce BCA Protein Assay kit	Thermo Fisher Scientific	Cat#23225
QIAquick PCR purification kit	QIAGEN	Cat#28104
RNeasy mini kit	QIAGEN	Cat#74106
Experimental Models: Cell Lines		
BCL2 dependent SVEC cell line	Lopez et al., 2016	NA
BCL-X_L dependent SVEC cell line	Lopez et al., 2016	NA
HeLa S3	Matheisl et al., 2015	NA
MCL-1 dependent SVEC cell line	Lopez et al., 2016	NA
Experimental Models: Organisms/Strains		
Human PBMCs	See Methods Details	NA
Nlrp3$^{-/-}$ mice	Mariathasan et al., 2006	NA
Asc$^{-/-}$ mice	Mariathasan et al., 2004	NA
Casp1/11$^{-/-}$ mice	Kuida et al., 1995	NA
Casp8$^{-/-}$/*Ripk3*$^{-/-}$ bone marrow	Kaiser et al., 2011	NA
Ripk3$^{-/-}$ bone marrow	Newton et al., 2004	NA
OXP-BCL2 mice	Knittel et al., 2016	NA
Bax$^{-/-}$/*Bak1*$^{-/-}$ bone marrow	Vince et al., 2012	NA
Gsdmd$^{-/-}$ bone marrow	Schneider et al., 2017	NA
Oligonucleotides		
Primer: *Hprt* Forward: CTGGTGAAAAGGACCTCTCG	Bieging et al., 2009	NA
Primer: *Hprt* Reverse: TGAAGTACTCATTATAGTCAAGGGCA	Bieging et al., 2009	NA
Primer *Mcl1* Forward: TGTAAGGACGAAACGGGACT	Austin and Cook, 2005	NA
Primer *Mcl1* Reverse: AAAGCCAGCAGCACATTTCT	Austin and Cook, 2005	NA
Recombinant DNA		
Hemoglobin subunit beta-pT7CFE1	This study	NA
Software and Algorithms		
GraphPad Prism 5	GraphPad	NA

CONTACT FOR REAGENT AND RESOURCE SHARING

Further information and requests for resources and reagents should be directed to and will be fulfilled by the Lead Contact, Veit Hornung (hornung@genzentrum.lmu.de).

EXPERIMENTAL MODEL AND SUBJECT DETAILS

Mice

All described mouse lines were housed under specific pathogen-free conditions. Animal housing and handling was conducted in accordance with the Principles of Laboratory Animal Care guidelines approved by the Local Animal Care Commission of North Rhine-Westphalia and supervised by Institutional Animal Care and Use Committee (IACUC) of the Medical Faculty, University of Bonn (HET, House of Experimental Therapy, University Hospital, University of Bonn). Mice were euthanized according to the FELASA guidelines by cervical dislocation. The gender of the individual mice was not documented for this study.

Preparation of murine bone marrow derived macrophages (BMDMs)

BMDMs were derived from bone marrow (BM) of 8-12 weeks old C57BL/6 mice. *Nlrp3*$^{-/-}$ (Mariathasan et al., 2006), *Pycard*$^{-/-}$ (Mariathasan et al., 2004) were kindly provided by Vishva Dixit (Genentech, USA), *Casp1/11*$^{-/-}$ (Kuida et al., 1995) were from Richard A. Flavell (Yale University, USA), bone marrow of *Casp8*$^{-/-}$/*Ripk3*$^{-/-}$ (Kaiser et al., 2011), *Ripk3*$^{-/-}$ (Newton et al., 2004) were a gift from

Egil Lien (UMASS Medical School). OXP-BCL2 mice (Knittel et al., 2016) were from Hamid Kashkar (University of Cologne, Germany). Bone marrow of *Bax*$^{-/-}$/*Bak1*$^{-/-}$ mice (Vince et al., 2012) was kindly provided by James Vince (WEHI, Australia), *Gsdmd*$^{-/-}$ (Schneider et al., 2017) from Petr Broz (University of Lausanne, Switzerland). Bone marrow cells were filtered and subjected to erythrocyte lysis (BD Pharm lyse). For the derivation of macrophages, bone marrow cells were supplemented with 30% L929 supernatant for 6-7 days. Cells were plated one night before the stimulation.

Isolation of human primary cells

PBMCs were isolated from heparinized blood or buffy coats from informed, consenting, and healthy volunteers according to the principles of the Declaration of Helsinki, approved by the responsible ethics committee (Ethics committee of the Medical Faculty, University of Bonn). Monocytes were isolated using CD14 MACS microbeads (Miltenyi Biotec) according to the manufacturer's protocol.

Primary cell culture

Human PBMCs and primary monocytes were cultured in RPMI medium 1640 supplemented with L-glutamine, sodium pyruvate, 10% (v/v) heat inactivated FCS and 100U/ml Penicillin-Streptomycin (all Life Technologies). Human PBMCs and monocytes (both at 1x10^5/well) were plated in 96 flat-well plate 2 h before the experiment. For Western Blot preparation, human monocytes (3x10^5/well) were seeded in 96 flat bottom plates with 3% FCS containing RPMI medium and samples from 5 wells were combined for each condition. All BMDMs were cultivated in DMEM supplemented with L-glutamine with same additive as above. BMDMs cells (1x10^6) were plated either in 12 well plates or 1x10^5 cells in 96 flat bottom plates/well. Primary MEFs were cultured in DMEM medium with 10% (v/v) heat inactivated FCS and 100U/ml Penicillin-Streptomycin along with 1% non-essential amino acids (all Life Technologies) and 100 μM β-Mercaptoethanol (Sigma Aldrich).

Cell lines

SVEC cells were cultured in DMEM medium containing 10% FCS and 2 mM Glutamine. HeLa S3 cells were grown to a density of 3.0–5.5 × 10^5 in SMEM (Sigma), supplemented with 10% FCS (GIBCO), Penicillin (100 U/ml) and 1x GlutaMAX (GIBCO) at 37°C, 5% CO2 using a spinner flask (40 rpm).

METHODS DETAILS

Cell stimulation

If not indicated otherwise, BMDMs cells were primed with 200 ng/ml ultrapure *E.coli* LPS (Invivogen) for 4 h. For dsDNA stimulation, 1 μg/ml of pBlueScript Plasmid DNA, isolated from *E. coli* with a Maxiprep Kit (Invitrogen) were complexed to Lipofectamine 2000 (Life Technologies) according to manufacturer's protocol, and cells were stimulated with the mix for 8 h. If not stated otherwise, Vio A, B, C and D (purified as previously described (Yan et al., 2018)) were used at 20 μM, nigericin (Sigma-Aldrich), birinapant (Biovision) and staurosporine (Santa Cruz) were added at final 6.5 μM, 20 μM and 1 μM concentrations, respectively, for 8 h. Inhibitors: MG-132 (Selleck chemicals), cycloheximide (Carl Roth), MCC950 (Tocris bioscience) and ABT-737 (Santa cruz) were used at 12.5 μM, 1μg/ml, 10 μM and 1 μM, respectively. In mito-priming assay, cells were stimulated with 1 μM concentration of either ABT-199 (BCL2i) or A-1155463 (BCL-X$_L$i) or S63845 (MCL-1i) specific inhibitor for BCL2, BCL-X$_L$ and MCL-1, respectively or with mentioned vioprolides concentrations. For high extracellular K$^+$ concentration, cells were incubated in medium that was diluted with 150 mM KCl (Roth) in sterile water to contain indicated concentrations of K$^+$ in the medium (Gaidt et al., 2016).

Immunoblotting, LDH and ELISA assay

BMDMs cells were plated in 12 well plates for immunoblots. Next day, cells were stimulated in 1% FCS medium for indicated times. Supernatants were taken separately from 12 well plate for IL-1β ELISA (50 μl) (BD bioscience) and LDH (40 μl) (Thermo scientific), performed according to manufacturer's instructions. LDH is depicted as a percentage relative to direct cell lysis It was calculated as LDH release (%) = 100 * (measurement – unstimulated control)/ (direct lysis control – unstimulated control). Remaining supernatants were precipitated and resuspended in 1X SDS laemmli buffer (Jakobs et al., 2013). Cells were lysed directly on plates in 1X SDS laemmli buffer. Samples were heated at 95°C with 1100 rpm and loaded on SDS-PAGE gel (5% stacking gel and 12% separating gel; BioRad). Afterward, proteins were transferred on nitrocellulose membrane (Amersham, GE healthcare) for 1 h. Membranes were blocked for another 60 min in 3% milk in PBST (PBS containing 0.05% Tween 20). All primary antibodies were incubated at least overnight in 1% milk in PBST at 4°C. Next day, membranes were incubated for at least 1 h in secondary antibody and washed gently in PBST buffer for further 30-60 min. Chemiluminescent signal was recorded with CCD camera in Fusion SL (PEQLAB). In some blots, whole image was contrast-enhanced in a linear fashion.

Quantitative PCR

BMDMs (7x10^5) were plated in 12 well plates and stimulated for 4 h. Cells were lysed in RLT buffer. Total RNA was isolated using RNeasy mini kit from QIAGEN (74106) followed by DNase I (Thermo Fisher Scientific, EN0525) treatment. Afterward, cDNA was prepared using RevertAid RT (Thermo, EP0441) using supplier's instructions. Real time PCR was performed using Fast SYBR green

(Thermo Fisher Scientific, 4385618) according to manufacturer's instructions. *Hprt* (Fwd primer: 5′-CTGGTGAAAAGGACCTCTCG-3′ and Rev primer: 5′-TGAAGTACTCATTATAGTCAAGGGCA-3′) (Bieging et al., 2009) was used as endogenous control. Expression of *Mcl1* was measured using Fwd primer: 5′-TGTAAGGACGAAACGGGACT-3′ and Rev primer: 5′-AAAGCCAGCAGCACATTTCT-3′ (Austin and Cook, 2005).

Cytoplasmic extraction of BMDMs

BMDMs were plated at 6-8x10^6 cells per well in 6 well plate. Medium was replaced with fresh pre-warm medium with 1% FCS. After stimulation, medium was removed and cells were washed with PBS. Cells were lysed with buffer A (250 mM sucrose, 10 mM HEPES pH 7.8, 10 mM KCl, 2 mM $MgCl_2$, 0.1 mM EGTA, 1mM DTT, 0.1% NP-40, complete protease inhibitor cocktail and 0.5 mM PMSF). To remove cell nuclei, lysates were centrifuged at 700 g for 15 min. Supernatants were taken and centrifuged again for 20 min at 12000 g (modified from (Park et al., 2013)). Resulting supernatants were used as cytoplasmic fraction and protein concentrations were measured with BCA kit (Pierce protein assay kit). Measured samples were mixed with 6X SDS laemmli buffer before running on SDS-PAGE gels. Beta actin was used as loading control. COXIV was used as control for mitochondrial contamination in cytoplasmic samples.

DNA laddering assay

BMDMs (2x10^6) were plated in 12 well-plate for each condition. DNA laddering assay was performed as described previously with some changes (Kralj et al., 2003). Briefly, after stimulation cells were washed with PBS and lysed in 200 μl of lysis buffer (1% NP-40 in 20 mM EDTA, 50 mM Tris-HCl, pH 7.5). samples were centrifuged at 3000 rpm for 5 min and supernatants were collected. SDS (1%) and RNase A (5 μg/ml) were added for 1 h at 56°C. it was followed proteinase K (2.5 μg/ml) treatment for 1 at 37°C. Afterward, ½ volume of ammonium acetate (stock 10 M), 2 volume of ice cold ethanol and small amount of glycogen were added to the samples. It was followed by incubated at −80°C overnight for precipitation. Next day, after centrifugation (14000 rpm) for 40 min at 4°C, pellets were washed with 70% ethanol and dissolved in 20 μl of water. Equal amounts of DNA were loaded for each condition on a 2% agarose gel.

Plasmid preparation for hemoglobin subunit beta (HBB)

The HBB construct was cloned into the pT7CFE1 backbone as described previously (Matheisl et al., 2015). Sequence of mRNA construct:

ATGgcccaccaccaccaccaccacctggccaccacccatatgCTGGAAGTGCTGTTTCAGGGCCCGtacccatacgatgttccagattacgctGTGCATC
TGACTCCTGAGGAGAAGTCTGCCGTTACTGCCCTGTGGGGCAAGGTGAACGTGGATGAAGTTGGTGGTGAGGCCCTGGGCAG
GCTGCTGGTGGTCTACCCTTGGACCCAGAGGTTCTTTGAGTCCTTTGGGGATCTGTCCACTCCTGATGCTGTTATGGGCAACCC
TAAGGTGAAGGCTCATGGCAAGAAAGTGCTCGGTGCCTTTAGTGATGGCCTGGCTCACCTGGACAACCTCAAGGGCACCTTTG
CCACACTGAGTGAGCTGCACTGTGACAAGCTGCACGTGGATCCTGAGAACTTCAGGCTCCTGGGCAACGTGCTGGTCTGTGTG
CTGGCCCATCACTTTGGCAAAGAATTCACCCCACCAGTGCAGGCTGCCTATCAGAAAGTGGTGGCTGGTGTGGCTAATGCCCT
GGCCCACAAGTATCACTAA

Human *in vitro* translation extract

As described previously (Matheisl et al., 2015), The translation extract was prepared using HeLa S3 cells. In brief, HeLa S3 cells were harvested (2 min, 650 g) and the pellet was washed 3 times with washing Buffer (35 mM HEPES/KOH pH 7.5, 140 mM NaCl, 11 mM Glucose) (1 min, 650 g) and 1x with extraction Buffer (20 mM HEPES/KOH pH 7.5/4°C, 45 mM KOAc, 45 mM KCl, 1.8 mM $Mg(OAc)_2$, 1 mM DTT). Next, the cell pellet was resuspended in extraction Buffer (1.2 × 10^9 cells/ml) and disrupted by nitrogen pressure (300 psi, 30 min, 4°C) in a cell disruption vessel (Parr Instrument). Next, the lysate was mixed with 1/29 volume high potassium buffer (20 mM HEPES/KOH pH 7.5/4°C, 945 mM KOAc, 945 mM KCl, 1.8 mM $Mg(OAc)_2$, 1 mM DTT) and incubated at 4°C for 5 min, followed by brief centrifugation step (20 s, 14 000 rpm, 4°C). Aliquots of the resulting supernatant were frozen in liquid nitrogen and stored at −80°C.

In vitro transcription

In vitro transcription was performed as previously with some minor changes (Matheisl et al., 2015). Plasmid was linearized with SpeI-HF (NEB) in CutSmart (NEB) buffer at 37°C overnight and purified by QIAquick PCR purification kit (QIAGEN) before *in vitro* transcription (tc) to ensure the right length of the mRNA product. The final mRNA construct encoded a CrPV IGR IRES sequence for translation initiation, an N-terminal HA- and (His)6-tag, the human HBB sequence and a polyA-tail. The reaction was performed in tc buffer (40 mM Tris/HCl pH 7.9/4°C, 26 mM $MgCl_2$, 0.01% Triton X-100, 2.5 mM Spermidine, 5 mM DTT, 6.25 mM ATP, 6.25 mM CTP, 6.25 mM GTP, 6.25 mM UTP, 0.2 U/ml RNasin (Ambion)) with home-made T7 RNA polymerase and 1.5 μg linearized plasmid per 100 μL reaction was used. The tc reaction was incubated for 4 h at 37°C. Additional amount of T7 RNA polymerase was added during incubation. The resulting mRNA was purified by LiCl precipitation method and stored at −80°C.

In vitro translation

In vitro translation (tl) was performed in tl buffer (14 mM HEPES/KOH pH 7.5/4°C, 135 mM KOAc, 20.1 mM KCl, 31 mM $Mg(OAc)_2$, 2 mM DTT, 0.25 mM GTP, 1.56 mM ATP, 16 mM Creatine Phosphate (Roche), 0.45 μg/μl Creatine Kinase (Roche), 50 μg/ml yeast tRNA, 0.4 mM Spermidine) with 50% (v/v) extract. This mixture was supplemented with 0.12 mM amino-acid mixture, complete (Promega) and 0.885 U/μl RNasin (Ambion). 1 μg mRNA/12 μL translation reactions were added before incubation for 40 min at 30°C (modified from (Matheisl et al., 2015)). Reactions were terminated using 1X SDS laemmli buffer and samples were heated for 5 min at 65°C before loading of SDS-PAGE gel. Samples were probed using anti-HA antibody (H6908) from Sigma.

Mito-priming Assay

Mitoprimed SVEC cells (Lopez et al., 2016) expressing eGFP-tBID 2A Bcl-2, eGFP-tBID 2A Bcl-X_L or eGFP-tBID 2A Mcl-1 were seeded in 24 well plates ($3x10^4$ cells/well) overnight. The following day, cells were treated in the presence of 30 nM Sytox Green (Life Technologies) together with the indicated compounds and imaged using an Incucyte FLR instrument (Essen Bioscience). Four images per well were acquired every hour, and the number of Sytox green positive cells per mm^2 were determined. Results were normalized to the initial confluency of each well.

QUANTIFICATION AND STATISTICAL ANALYSIS

Statistical analysis

If not stated otherwise, data are presented as mean values of the indicated number of independently conducted experiments, whereas the error bars represent the standard error of mean (SEM). If indicated, data were analyzed for statistically significant differences using Two-way ANOVA or One-way ANOVA using Bonferoni's correction for multiple testing if multiple conditions or experimental groups were to be compared. Gaussian distribution and sphericity of datasets were assumed. For qPCR, logarithmic values were used to obtain a normal distribution before performing statistics. Time course experiments in mito-primed cells were evaluated using the Kruskal-Wallis H test (non-parametric one-way ANOVA) and posthoc analysis with Dunn's multiple comparison test. The statistical analysis was performed using GraphPad. ** $p < 0.01$, * $p < 0.05$, ns = not significant.

DATA AND SOFTWARE AVAILABILITY

All the original immunoblots images can be found on Mendeley using this link: https://doi.org/10.17632/5889f7w6s8.1